2007

High- and Ultrahigh-Pressure Metamorphism in the North Qaidam and South Altyn Terranes, Western China

Chris G. Mattinson
Stanford University, mattinson@geology.cwu.edu

C. A. Menold
Albion College

Jian-Xin Zhang
Chinese Academy of Geological Sciences

D. K. Bird
Stanford University

Recommended Citation

Mattinson, C.G., Menold, C.A, Zhang, J.X. and Bird, D.K. (2007). High and ultrahigh-pressure metamorphism in the North Qaidam and South Altyn terranes, Western China. *International Geology Review, 49*(11), 969-995. DOI: 10.2747/0020-6814.49.11.969

Citation: Mattinson, C.G., Menold, C.A., Zhang, J.X., and Bird, D.K. (2007) High- and Ultrahigh-Pressure Metamorphism in the North Qaidam and South Altyn Terranes, Western China. International Geology Review, 49(11), 969-995.

High and ultra-high pressure metamorphism in the North Qaidam and South Altyn terranes, Western China

C.G. Mattinson[1], C.A. Menold[2], J.X. Zhang[3], and D.K. Bird[1]

[1]Department of Geological & Environmental Sciences, Stanford University, Stanford CA 94305-2115 U.S.A.

[2]Department of Geology, Albion College, Albion MI 49224, U.S.A.

[3]Chinese Academy of Geological Sciences, Institute of Geology, Beijing 100037, China

Abstract

The North Qaidam and South Altyn terranes extend approximately 1000 km across the northern Tibetan Plateau, and five localities preserve evidence of Early Paleozoic high-pressure (HP) or ultra-high pressure (UHP) metamorphism, including the presence of coesite, coesite pseudomorphs, and diamond. A review of the geology, petrology, and geochronology collected over the past ten years since these localities were discovered supports a correlation of the North Qaidam and South Altyn terranes, offset 350–400 km across the Altyn Tagh fault. Geochronology interpreted to reflect eclogite-facies metamorphism yields ages between 500 and 420 Ma; detailed geochronology from one locality supports a protracted (10s of Ma) history of HP/UHP metamorphism. Rock associations and geochronology support a passive margin origin for the protolith of the HP/UHP rocks, which received sediments from a Proterozoic–Late Archean source, and was intruded by Neoproterozoic granites derived from crustal melting.

Introduction

Ultra-high pressure (UHP) metamorphism, defined by the pressure-temperature conditions of the coesite stability field (P > 27 kbar, depths > 80 km), is a product of continental subduction and collision (Coleman and Wang, 1995). Since the discovery of metamorphic coesite (Chopin, 1984; Smith, 1984) and diamond (Sobolev and Shatsky, 1990), UHP terranes have been documented from more than 15 localities (e.g., Liou et al., 2002). Typically, evidence of UHP metamorphism is preserved as rare mineral inclusions or relict mineral assemblages within host rocks that reequilibrated at crustal conditions. Western China contains several high-pressure (HP) metamorphic belts; evidence for UHP metamorphism has been documented from the North Qaidam and South Altyn terranes (Fig. 1). In contrast to the well-studied Qinling-Dabie-Sulu belt (Fig. 1; e.g., Ernst and Liou, 2000), the recently discovered North Qaidam and South Altyn terranes are less well explored. Here we review the petrology and geochronology collected from these belts over the past ten years, and assess the constraints these data place on tectonic models of Western China.

Geologic setting of the North Qaidam terrane

The North Qaidam HP/UHP terrane is a major, northwest-southeast trending, early Paleozoic continental suture zone in central Asia (Fig. 1), bounded on the southwest by the Qaidam Basin, and on the northeast by the Qilian terrane (Fig. 1b; Yang et al., 2001c). The Altyn Tagh fault truncates the northwestern end of the terrane, and the southeastern end is truncated by the Wenquan fault. Correlation of the Qaidam terrane to the northwest of the Altyn Tagh fault remains a subject of active research, but the

evidence we review here supports a correlation with the South Altyn terrane (Fig. 1; described below). To the southeast, the relatively minor offset of the Wenquan fault (Fig. 1b; Wang and Burchfiel, 2004) separates the North Qaidam terrane from the Gonghe basin, and connections between the North Qaidam terrane and the west Qinling belt remain to be explored.

The basement of the North Qaidam terrane is the Proterozoic Dakendaban Group gneiss, which is overlain by Paleozoic metasediments (locally in thrust contact with the gneiss), and intruded by granites (BGMQ, 1991). The Dakendaban Group includes paragneiss, orthogneiss, marble, amphibolite, migmatite, and locally eclogite and ultramafic rocks including garnet peridotite (Yang et al., 1994, 1998, 2001a, c). Eclogite occurs in three localities over a distance of 350 km; from southeast to northwest these are Dulan, Xitie Shan, and Lüliang Shan. Their locations are shown on Figure 1b, and geologic maps are presented in Figures 2–4. The eclogite and peridotite occur as blocks, boudins or layers in the host para- and orthogneiss, and typically are 10s to <1m across, but locally are up to 100s of m across.

The Dakendaban gneiss is dominated by metagranitic and metasedimentary rocks. Field relations, including inclusions of metasediments in metagranite (Wan et al., in press) and intercalation of granitic and sedimentary gneiss, suggest that the metasediments were intruded by the granite, and therefore sediments are >1 Ga (see below). Neodymium depleted-mantle model ages from the metasediments are predominantly 1.9–2.2 Ga (Wan et al., in press), and should approximate the formation age of the parent rocks from which the sediments were derived. This suggests the sediments were derived from Paleoproterozoic ± Archean crustal material, consistent

with analyses of zircon cores from paragneiss (see below); a passive margin depositional environment is suggested by Wan et al. (in press). Metagranite Nd depleted-mantle model ages of 2.0–2.4 Ga are similar to those of metasediments, which indicates that the granites were derived from partial melting of continental crust, possibly the metasediments into which they intrude (Wan et al., in press). This is consistent with ~2.5 Ga inherited zircon in granitic gneiss (Mattinson et al., 2006) and oxygen isotope values of +14–15 (C.A. Menold, unpubl. data). Wan et al. (in press) suggest that the granites were formed during the assembly of Rodinia.

Paleozoic granites cross-cut the regional foliation, and crystallized between 397–456 Ma, which is considered to be coeval with continental collision between the North Qaidam and Qilian terranes (Gehrels et al., 2003b; Wu et al., 2001, 2004). North of the North Qaidam terrane, granites in the southern Qilian terrane (Fig. 1) have I-type geochemistry, 425–496 Ma ages, and are interpreted to represent arc magmatism (Gehrels et al., 2003b; Wu et al., 2001). The subduction polarity responsible for convergence, magmatism, and subsequent collision of the North Qaidam and Qilian terranes is unclear, and models involving both north-dipping subduction (Song et al., 2006; Yang et al., 2001c, 2002; Yin and Harrison, 2000) and south-dipping subduction (Gehrels et al., 2003a, b; Sobel and Arnaud, 1999) have been proposed (see discussion section). Additional field and geochronological work is required to resolve this problem. All rock types were subsequently uplifted and eroded during Cenozoic deformation associated with the India-Asia collision.

Below we present an overview of the geology at Dulan, Xitie Shan, and Lüliang Shan in the North Qaidam terrane, and Bashiwake and Jianggalesayi in the South Altyn

terrane. Tables 1 and 2 compile thermobarometry and geochronology from journal publications, meeting abstracts, and our unpublished data. These data are summarized in Figures 5–14.

Dulan

This region, named for the town of Dulan, located approximately 30 km southwest of the map area in Fig. 2, is also known as the Shaliuhe area, after the Shaliu River which flows through the map area. Eclogite and ultramafic rocks occur within the Dakendaban Group gneiss (also known as the Shaliuhe Group in this region, Yang et al., 2000) both north and south of the Shaliu River, and Song et al. (2003a, b) subdivide outcrops in the Dulan area into a north belt (north of 36°32´) and a south belt. The Dakendaban gneisses include granitic gneiss, pelitic gneiss and schist, and minor marble and amphibolite. An amphibolite-facies foliation in the gneiss strikes northwest, and dips steeply northeast, modified by tight to isoclinal folds. A locally developed subhorizontal to shallowly northwest plunging lineation trends northwest. Layers and boudins of eclogite and ultramafic rocks <1 to 10s of m long are enclosed in both ortho- and paragneiss (Fig. 5a), and are aligned with the foliation in the surrounding gneiss; where developed, foliation within the layers is also concordant with the surrounding gneiss. Granite and granodiorite of the Yematan batholith (Fig. 2) cross-cut the foliation in the Dakendaban gneiss (Fig. 5b), indicating that ductile deformation had ceased prior to intrusion, and yield major and trace element signatures intermediate between I- and S-type, which Wu et al. (2001, 2004) interpret to reflect a post-collisional origin.

Petrology and thermobarometry

The Dakendaban gneisses are dominated by pelitic schist and gneiss with the assemblage Qtz + Mu ± Bt ± Grt ± opq ± Kfs ± Pl ± Tur ± Ky (mineral abbreviations follow Kretz, 1983, except phengite, Phe, and opaque minerals, opq), and by granitic orthogneiss, commonly with Kfs augen, with the assemblage Qtz + Kfs + Pl + Bt ± Mu ± Grt ± Tur. Garnet is common in paragneiss, but is rare in orthogneiss; accessory tourmaline is common in both rock types. Minor rock types include biotite-quartzite, with the assemblage Qtz + Bt ± Mu ± Grt; marble with trace Phl/Tlc ± Grt ± Spn; and calc-silicate with the assemblage Cal + Ep + Grt + Spn.

Eclogite (Fig. 5c) contains the assemblage Grt + Omp + Rt ± Qtz ± Ep ± Phe; samples in the south belt additionally contain kyanite, reflecting their higher Al_2O_3 bulk composition (Song et al., 2003a). In retrogressed samples green amphibole is also present, and omphacite is replaced by symplectites of oligoclase + sodic augite or amphibole + albite, and biotite + plagioclase intergrowths may represent former phengite. Amphibolite contains Amp + Pl + Spn ± Qtz ± Grt ± opq ± Ep, and the presence of rutile in some samples suggests that these are retrogressed eclogites.

Most ultramafic rocks are strongly serpentinized to an assemblage of Srp + opq ± Chl ± Tlc ± Ol ± Cpx; serpentinites represent both dunite and peridotite. One sample contains a garnet peridotite assemblage of Ol + Opx + Cpx + Grt (Fig. 5d); serpentine partially replaces olivine and pyroxene, and garnet is largely replaced by green-brown spinel. Clinopyroxenites contain the assemblage Cpx + opq ± Chl ± Srp ± Grt. Several samples with the assemblage Cpx + Chr + Chl ± Amp contain large (>5 mm) Cpx porphyroclasts (Fig. 5e) that contain exsolved Cr-rich spinel or Cr-magnetite + Cr-

chlorite ± trace phlogopite (Mattinson et al., 2003). Chlorite in these samples appears to be in equilibrium with fine-grained clinopyroxene in the matrix and inclusion-free porphyroblast rims (Fig. 5e).

Song et al. (2003a, b) report peak pressure-temperature (P-T) conditions (Fig. 6; Table 1) for eclogites of 29–32 kbar, 631–687°C (north belt) and 29–33 kbar, 729–746°C (south belt), and interpret polycrystalline quartz inclusions in garnet and omphacite to represent coesite pseudomorphs. Raman spectroscopic identification of coesite included in zircon from the host paragneiss confirms that both the mafic/ultramafic rocks and the felsic host gneiss were metamorphosed at UHP conditions (Song et al., 2001a, b, 2003b, 2006; Yang et al., 2001a). The prograde path is unconstrained by thermobarometry, but blocky, polycrystalline clinozoisite inclusions in the cores of eclogite garnets may represent lawsonite pseudomorphs (Mattinson et al., in press), which suggests a low geothermal gradient during prograde subduction of the UHP rocks (e.g., Poli and Schmidt, 1995). Retrograde conditions are not quantitatively constrained for the north belt eclogites, but Song et al. (2003b) suggest that Cpx + Pl and Hbl + Ab symplectite rims around omphacite indicate near-isothermal decompression to amphibolite-facies conditions (Fig. 6). A more complete record of metamorphic conditions during exhumation is provided by south belt eclogites: growth of coarse-grained plagioclase, low-Na clinopyroxene, and sulfate-bearing scapolite records granulite-facies (19–20 kbar, 873–948°C) conditions, and the assemblage Hbl + Ep + Pl + Bt + Qtz records amphibolite-facies (7–9 kbar, 660–695°C) conditions (Fig. 6; Song et al., 2003b). Song et al. (2003b) suggest different tectonic settings, with slower exhumation in the south belt, to produce the different P-T paths in the two belts. However, it is unclear if high

temperatures during decompression can be excluded for the north belt, or if development of a granulite-facies assemblage was impeded by the different bulk composition or lack of catalyzing fluid.

Geochronology

Geochronology results for the Dulan region are compiled in Table 2, and results interpreted to reflect the Early Paleozoic high-pressure event are summarized in Figure 7. Only two analyses have been performed of eclogite from the south belt, and both appear to be older than the other published analyses. However, the Sm/Nd age is imprecise due to a low Sm/Nd ratio in the garnet fraction, and lack of colinearity of whole-rock, omphacite, and garnet suggests disequilibrium and therefore the isochron may not accurately represent the age of metamorphism (Song et al., 2003a). The U/Pb age is from TIMS analysis, which will yield an average age if the zircons are internally complex, as we observe for samples from the north belt. Further work is needed in order to determine if there is a true age difference between the two belts.

Analyses of eclogite from the north belt reveal a range of ages from 459 to 422 Ma (Fig. 7 and Table 2). The U/Pb ages represent eclogite-facies zircon growth based on inclusions of garnet, omphacite, and rutile, and also by rare-earth element (REE) patterns (Mattinson et al., in press; Song et al., 2006) characterized by heavy REE depletion without a negative Eu-anomaly, due to the presence of abundant garnet and the absence of plagioclase (e.g., Rubatto, 2002). These observations led Mattinson et al. (in press) to conclude that these rocks remained in the eclogite-facies for 25 m.y. or more. Analyses of metamorphic zircon in paragneisses show a similar age range (Fig. 7; Table 2), and

individual spot analyses of coesite-bearing zircon grains suggest UHP conditions at ca. 425 Ma, and possibly as early as 440 Ma (Fig. 7, Table 2).

Constraints on the timing of retrograde metamorphism and exhumation include zircon rim ages from eclogite and gneiss, and a 402 Ma muscovite $^{40}Ar/^{39}Ar$ age (Fig. 7; Table 2, Song et al., 2006; Yang et al., 2005). These results suggest the UHP rocks reached mid- to shallow crustal levels at or before this time. The undeformed, cross-cutting granite and granodiorite of the Yematan batholith (Fig. 2) indicates that ductile deformation ceased before crystallization of the batholith at 397 ±3 Ma (Wu et al., 2001, 2004).

The protolith age of the eclogites is not well constrained. Lu (2003) reports a discordant Pb/Pb zircon age as old as 1482 Ma from the south belt, and an upper intercept age from this sample is 2055 Ma (Table 2). Mattinson et al. (in press) report zircon cores from eclogite as old as 474 Ma; based on inclusions and REE patterns, these ages represent prograde (?) metamorphic growth below the eclogite-facies. Zircon cores from paragneiss are as old as ~2.5 Ga. Fifteen analyses plotted in Figure 8 reveal relative probability peaks at 2.5 Ga and 1.9 Ga, suggesting that these sediments were sourced from Paleoproterozoic to Archean crust. Similar age peaks in the North China craton (Fig. 8; Kusky and Li, 2003) suggest that the North China craton may be a source for the sediments, although minor Paleoproterozoic to Archean rocks are also known from the Yangtze craton (e.g., Zheng et al., 2006). Analyses of two granitic orthogneiss samples indicate magmatic crystallization at ca. 925 Ma (Table 2), and ages from zircon rims (397–487 Ma) are compatible with minor recrystallization during in-situ metamorphism of the eclogite and paragneiss (Mattinson et al., 2006).

Xitie Shan

The Xitie Shan region, named for the mountain range containing the eclogite blocks, is located approximately 200 km west of Dulan (Fig. 1b). Eclogite and ultramafic rocks occur within the Dakendaban Group gneiss (Zhang et al., 2005c). The Dakendaban gneisses include granitic gneiss, pelitic gneiss and schist, and minor marble and amphibolite. An amphibolite-facies foliation in the gneiss strikes northwest, and dips steeply northeast, modified by SSE-NNW trending folds. Locally developed sub-horizontal stretching lineations are defined by biotite and sillimanite. Layers and boudins of eclogite and ultramafic rocks <1 to 10s of m long are enclosed in both ortho- and paragneiss, and are aligned with the foliation in the surrounding gneiss; where developed, foliation in the edges of eclogite blocks is also concordant with that of the surrounding gneiss.

Petrology and thermobarometry

The Dakendaban gneisses are dominated by granitic orthogneiss, commonly with Kfs augen, with the assemblage Qtz + Kfs + Pl + Bt ± Mu ± rare Tur, and by pelitic schist and gneiss with the assemblage Qtz + Mu ± Bt ± Grt ± opq ± Kfs ± Pl ± Ky ± Sill. Eclogite contains the assemblage Grt + Omp + Rt + Qtz in the center of large blocks. In the retrogressed edges of blocks green amphibole is also present, and omphacite is replaced by symplectites of andesine + diopside. Amphibolite contains Amp + Pl + Spn ± Qtz ± Grt ± opq ± Ep, and the presence of rutile in some samples suggests that these are retrogressed eclogites.

Zhang et al. (2005c) report peak pressure-temperature (P-T) conditions (Fig. 9; Table 1) for eclogites of >14 kbar, 730-830°C, well below UHP conditions. Retrograde conditions are further constrained by growth of coarse-grained plagioclase, low-Na clinopyroxene, and garnet recording granulite-facies (10–15 kbar, 750–865°C) conditions. No evidence of a prograde assemblage has been identified in this locality.

Geochronology

Geochronology results for the Xitie Shan region are compiled in Table 2, and results interpreted to reflect the Early Paleozoic high-pressure event are summarized in Figure 10. The U/Pb age of eclogitic zircon was calculated by SHRIMP analysis and by TIMS analysis, which will yield an average age if the zircons are internally complex. Ages calculated from both methods overlap with in error with ~486 Ma interpreted to be the age of metamorphic zircon growth (Zhang et al., 2005c). A Sm/Nd age of 436 ± 49 Ma was obtained by Zhang et al. (2005c) for eclogite but it is imprecise due to a lack of colinearity of whole-rock, omphacite, and garnet suggesting disequilibrium in the sample. This method dates late eclogite facies metamorphism in the area as all the minerals analyzed recrystallized during the high temperature retrograde event. $^{40}Ar/^{39}Ar$ analysis of a single pargasitic amphibole sample yields a cooling age of 407 ± 4 Ma (Zhang et al., 2005c)

Constraints on the timing of retrograde metamorphism and exhumation of the eclogite-bearing gneiss to mid-crustal conditions include a 486 Ma zircon age, an imprecise 436 Ma Sm/Nd age and a 407 Ma amphibole $^{40}Ar/^{39}Ar$ age (Table 2, Figure 10) (Zhang et al., 2005c). The protolith age of the eclogites is not well constrained. Two

SHRIMP analyses of CL dark cores yield discordant ages of 755 and 768 Ma which overlap the upper intercept of TIMS analyses, and are interpreted to reflect the protolith age of the eclogite (Zhang et al., 2005c).

Lüliang Shan

The Lüliang Shan region, named for the mountain range containing the eclogite blocks, is located approximately 50 km northwest of Xitie Shan, and is also known as the Yuka area, after the Yuka river located on the northern flank of the Lüliang Shan range (Fig. 1b, 4). Eclogite and ultramafic rocks occur within the Dakendaban Group gneiss (Li et al., 1999). The Dakendaban gneisses include granitic gneiss, pelitic gneiss and schist, and minor marble and amphibolite. A pervasive amphibolite-facies deformation event imparted a common sub-horizontal to steeply-dipping foliation on all units, and folded and transposed tectonic contacts. Removal of the effects of Cenozoic deformation suggests that the foliation was originally sub-horizontal. The foliation of the eclogite rims matches the regional amphibolite-facies fabric found in the surrounding gneiss and throughout the North Qaidam metamorphic belt. Discrete shear zones, 2-5 m thick, with top-N and top-NE sense of kinematic indicators, are locally present near contacts with epidote-amphibolite facies Paleozoic ophiolite complex rocks (gabbro, plagiogranite, mafic dikes, vesicular basalt, and metasediments).

In this locality, layers and boudins of eclogite and ultramafic rocks <1 to 100s of m long are enclosed in granitic gneiss. Early Silurian granite and granodiorite (Fig. 3) cross-cut the foliation in the Dakendaban gneisses, indicating that ductile deformation

had ceased prior to intrusion, and yield I-type major and trace element signatures indicative of arc magmatism (Menold, unpubl. data).

Petrology and thermobarometry

The Dakendaban gneiss in this locality is dominated by granitic orthogneiss, commonly with Kfs augen, with the assemblage Qtz + Kfs + Pl + Mu ± Pg ± Bt ± Grt ± Tur. Garnet is rare in orthogneiss, occurring mainly in proximity to eclogite blocks. In the northern Lüliang Shan, pelitic rocks locally contain an eclogite-facies assemblage of Grt + Phe + Ky + Cld + Pg + Qtz (Zhang et al., 2004a). Minor rock types include biotite-quartzite, with the assemblage Qtz + Bt ± Mu ± Grt; marble with trace Phl/Tlc ± Grt ± Spn.

Eclogite contains the assemblage Grt + Omp + Rt ± Qtz ± Ep ± Phe. All eclogite blocks have amphibolite-facies rims containing green amphibole with omphacite replaced by symplectites of oligoclase + sodic augite or amphibole + albite, and biotite + plagioclase intergrowths may represent former phengite. Amphibolite contains Amp + Pl + Spn ± Qtz ± Grt ± opq ± Ep, and the presence of rutile in some samples suggests that these are retrogressed eclogites.

In the southern part of the Lüliang Shan belt there is one occurrence of garnet peridotite, the largest observed garnet peridotite body in the North Qaidam metamorphic belt (500 x 1000 m^2) (Fig. 4). Layers of dunite (~15 vol%; Ol + Opx + Cpx ± Grt) are interlayered with the garnet peridotite (Ol + Grt + Cpx + Opx + Cr-rich Spinel) and veins of garnet pyroxenite (<5 vol%; Grt + Cpx + Opx + Phl) crosscut the body (Song et al.,

2004). No eclogite occurs with this ultramafic body, and paragneiss in the southern Lüliang Shan contains a granulite-facies assemblage of Grt + Sil + Bt + Kfs + Pl + Qtz.

A detailed pressure-temperature path has been determined for eclogites in the Lüliang Shan locality (Fig. 9). Using garnet inclusions in mafic eclogites, peak metamorphic pressures were calculated to be 25 ± 2 kbar at 650 ± 50 ºC, consistent with metamorphism near the coesite=quartz equilibrium (Zhang et al. 2004a; 2005c; Menold, unpubl. data). Li et al. (1999) reported coesite in the Lüliang Shan, but did not include photographs of the grains and the Raman spectra were inconclusive; this report has not been confirmed. The P-T data indicate slight heating during decompression from conditions of 26 kbar and 625 ºC to 6 kbar and 480 ºC, with temperature increasing slightly during initial decompression (Fig. 9) (Menold, unpubl. data). The pressure and temperature of the amphibolite assemblage observed in the rims of eclogite blocks was determined to be 425 ± 25˚C and 7-9 kbar. This is interpreted to be the P-T condition of the metamorphic event which generated the regional amphibolite fabric observed throughout the North Qaidam metamorphic belt.

Thermobarometry of garnet peridotite in the southern Lüliang Shan (Song et al., 2004, 2005) yields a higher pressure and temperature history than the nearby eclogite (Fig. 9; Table 1; Zhang et al., 2004a, 2005c). The garnet dunite and garnet lherzolite (Song et al., 2004, 2005) yielded peak conditions of 46-65 kbar, 980–1130 °C; garnet pyroxenite yielded conditions of 25–30 kbar, 800–900 °C (Fig. 9, Table 1). Based on the presence of plagioclase inferred from zircon REE patterns, and relatively Fe-rich olivine [Mg/(Mg + Fe) = 0.84–0.91], Song et al. (2005) concluded that the magnesite-bearing garnet lherzolite originated as a low-pressure crustal cumulate.

Geochronology

Geochronology results for the Lüliang region are compiled in Table 2, and results interpreted to reflect the Early Paleozoic high-pressure event are summarized in Figure 10. The U/Pb ages of zircon are from SIMS and TIMS analysis; analyses of zircon from eclogite reveal a range of ages from 488-800 Ma (Fig. 10 and Table 2) (Zhang et al., 2000; 2005c; Menold unpubl. data). The simplest explanation of the age spread is that the analyses represent a mixture between older cores (~800 Ma) and rims formed during Cambro-Ordovician UHP metamorphism. Given the large inherent uncertainties, a discordant system can not be ruled out a priori. U/Pb ages represent eclogite-facies zircon growth based on inclusions of garnet, omphacite, and rutile (Zhang et al., 2005c). Analyses of metamorphic zircon in orthogneisses also show a large age range (Fig. 10; Table 2).

Constraints on the timing of retrograde metamorphism and exhumation are provided by $^{40}Ar/^{39}Ar$ cooling ages on amphibole (477 ± 8 Ma) and muscovite (466-430 Ma) (Table 2; Menold et al., 2004; Zhang et al., 2005c); suggesting the UHP rocks reached mid- to shallow crustal levels at or before this time (Fig. 10). The undeformed, cross-cutting granite and granodiorite in both the north and south Lüliang Shan (Fig. 4) indicates that ductile deformation ceased before crystallization at 448 ± 3 Ma (Menold unpubl. data).

Zircon geochronology from the large garnet peridotite body in the southern Lüliang Shan (Fig. 4) yields distinctly younger ages of 420–423 Ma (Fig. 10; Table 2) that Song et al. (2005) interpreted to record UHP metamorphism based on REE patterns,

Grt + Ol inclusions, and one diamond inclusion, located at the boundary between the core and rim domains, identified by Raman spectroscopy. Zircon cores record ages of 446–457 Ma, and are interpreted by Song et al. (2005) to record magmatic crystallization, but a metamorphic origin cannot be excluded; two additional cores yield discordant, Proterozoic ages (Table 2). These data are difficult to reconcile with geochronology of the closely adjacent rocks: the felsic gneiss which hosts the peridotite records HP granulite-facies metamorphism at ~450 Ma, MP granulite-facies metamorphism at ~425 Ma (Zhang et al., in review), and cross-cutting granites yield ages of ~440 Ma (Menold unpubl. data) and 428 ± 10 Ma (Zhang et al., in review). Additional work is required to resolve the age of HP metamorphism in the southern Lüliang Shan and the relation between the garnet peridotite and the adjacent rocks.

The protolith age of the eclogite is not well constrained, but is interpreted to be ~800 Ma. The protolith age of the host orthogneiss is better constrained; this lithology typically contains abundant prismatic (~200 μm) zircons. In CL grains display oscillatory zoning consistent with an igneous origin and thin (<15 micron) unzoned rims interpreted to be metamorphic. Analyses from the core form a cord on a Concordia plot to ~950 Ma (Menold unpubl. data). TIMS analysis on abraded zircon grains yields a similar $^{238}U/^{206}Pb$ age of 928 ± 10 Ma (Gehrels et al., 2003b), interpreted to be the age of intrusion of the igneous protolith (Table 2; Fig. 14). Zircon geochronology of the ophiolitic rocks adjacent to the HP/UHP rocks yields 545.5 ± 6 Ma (Table 2; Menold et al., 2004).

Geologic setting of the South Altyn terrane

The Altyn Tagh, located at the northern edge of the Tibetan plateau, are separated from the Eastern Kunlun orogen and the Qaidam basin to the southeast by the Altyn Tagh fault, and are bounded on the west and north by the Tarim Basin (Fig. 1). E-W striking shear zones subdivide the range into four tectonic units (Sobel and Arnaud, 1999; Yang et al., 2001c; Zhang et al., 2005b). From NE to SW, these units are: (1) Archean (2.5–2.8 Ga) amphibolites and granulites of the Milan Group, Dunhuang massif (BGMX, 1993); (2) Early-Middle Paleozoic ophiolitic rocks (pillow lavas, serpentinite, mafic intrusives), locally including blocks of eclogite and blueschist (Zhang et al., 2005a) of the north Altyn suture (also known as the Lapeiquan suture or North Altyn Tagh subduction complex); (3) Mid- to Late Proterozoic felsic gneisses, marbles, amphibolites (Altyn Group), and continental margin metacarbonates (Jinyanshan Group) of the central Altyn block; and (4) Early Paleozoic (~500 Ma) eclogite, garnet peridotite, HP granulite, and amphibolite-facies gneiss of the south Altyn terrane (Liu et al., 2002; Zhang et al., 2001, 2002, 2005b). Evidence for HP/UHP metamorphism has been found in two locations within the south Altyn terrane, near Bashiwake in the eastern part of the terrane, and near Jianggalesayi (also spelled Jianggelesayi or Jianggeshayi), in the western part of the terrane (Fig. 1b)

Bashiwake

Near Bashiwake, sinistral strike-slip shear zones enclose a ~5 km wide HP/HT metamorphic unit within amphibolite-facies gneisses that lack evidence for HP metamorphism (Zhang et al., 2005b). Within the HP/HT unit, felsic granulites enclose

volumetrically minor (10s to 100s of m long) lenses and layers of metabasites and ultramafic rocks (Fig. 11). Quartz-bearing metabasites are enclosed directly within felsic granulite, and quartz-free metabasite layers occur within garnet peridotite. Ultramafic rocks include both garnet-free, strongly serpentinized layers up to 500 m long, and garnet-bearing, slightly serpentinized lenses <50 m wide.

Petrology and thermobarometry

The dominant rock type is felsic granulite, with a peak assemblage of Grt + Ky + ternary feldspar (now exsolved to mesoperthite) + Qtz (Zhang et al., 2005b). Kyanite is partially replaced by Spl + Pl ± Crn ± Grt, but sillimanite is absent. Quartz-bearing mafic granulite contains the peak assemblage Grt + Cpx + ternary feldspar (now exsolved to mesoperthite) + Qtz + Rt, and quartz-free mafic granulite contains the assemblage Grt + Cpx + Ky + Rt. Minor sapphirine, corundum, spinel, plagioclase, and amphibole appear to be secondary. Garnet peridotite contains the assemblage Grt + Ol + Opx + Cpx ± Mgs. Minor Chu, Dol, Spl, Amp, Chl, and Srp are also present, and many garnet grains are surrounded by Opx + Cpx + Spl kelyphites (Liu et al., 2002; Zhang et al., 2005b).

Thermobarometry of the different rock types yield similar peak metamorphic conditions of 18.5–27.3 kbar and 870–1020°C, and retrograde mineral assemblages are compatible with conditions of 9.4–12.2 kbar, 780–830°C determined from quartz-bearing mafic granulite (Fig. 12, Table 1). Thermobarometry from magnesite-bearing garnet lherzolite (Liu et al., 2002) yielded peak conditions of 38–51 kbar, 880–970°C (from grain cores), and 22–30 kbar, 710–800°C from grain rims (Fig. 12, Table 1). Based on spinel + amphibole inclusions in garnet, and Fe-rich olivine [Mg/(Mg + Fe) = 0.76–0.82],

Liu et al. (2002) concluded that the magnesite-bearing garnet lherzolite originated as a low-pressure crustal cumulate.

Geochronology

Zircon SHRIMP geochronology of felsic granulite, quartz-free mafic granulite, and garnet peridotite yield ages indistinguishable within error (Fig. 13; Table 2), consistent with HP metamorphic zircon growth at ca. 495 Ma (Zhang et al., 2005b). Discordant $^{207}Pb/^{206}Pb$ ages from felsic granulite zircon cores constrain the protolith age to >1722 Ma, and together with sample petrography are consistent with a metapsammitic protolith. However, zircon SHRIMP geochronology of another felsic granulite sample (Mattinson et al., 2005) indicates magmatic zircon growth at 925 ± 16 Ma, without evidence for Early Paleozoic metamorphic overgrowth, and indicates that some felsic granulite has a metagranitic protolith. Discordant $^{207}Pb/^{206}Pb$ ages from garnet peridotite zircon cores (Zhang et al., 2005b) constrain the protolith age to >1189 Ma.

Jianggalesayi

Eclogite cobbles in Pleistocene conglomerates and in modern stream channels were discovered by Hanson et al. (1995), and eclogite lenses in granitic and pelitic host gneiss were described by Chu (1998) and Zhang et al. (2001, 2002). Moderately to extensively retrogressed eclogite lenses a few cm to a few meters long occur in the host ortho- and paragneisses, and fresher eclogite is contained in stream cobbles (Chu, 1998; Zhang et al., 2001, 2002). The host rocks are primarily ortho- and paragneisses, with minor marble, calc-schist, and amphibolite (Yang et al. 2001c; Zhang et al., 2001). The

host gneisses contain garnet and sillimanite (locally kyanite), with local granulite-facies assemblages and incipient migmatization.

Petrology and thermobarometry

Eclogite contains a peak assemblage of Grt + Omp + Rt + Qtz ± Phe ± Zo. Garnet contains abundant inclusions of quartz and rutile, and sparse zoisite, amphibole and omphacite. Retrogression resulted in the growth of amphibole (5–25 vol%), replacement of omphacite by Cpx + Pl and Amp + Pl symplectites, and replacement of phengite by Bt + Pl symplectite (Chu, 1998; Zhang et al., 2001). Quartzofeldspathic host gneisses contain the assemblage Qtz + Kfs + Pl + Rt + opq, and amphibole gneiss contains the assemblage Amp + Ky + Kfs + Qtz + Pl + opq (Chu, 1998).

Thermobarometry on the eclogite-facies assemblage yields peak conditions of 28–30 kbar, 730–850°C (Fig. 12; Table 1), consistent with the interpretation that polycrystalline quartz inclusions in garnet represent coesite pseudomorphs (Zhang et al., 2001; 2002). Thermobarometry on the garnet (rim) + symplectite (clinopyroxene + plagioclase) + quartz assemblage yields 11–14 kbar, 670–800°C, and the amphibolite-facies assemblage yields 6.3–9.5 kbar, 619–738°C (Fig. 12; Table 1).

Geochronology

A garnet–omphacite–whole-rock Sm-Nd isochron yields 500 ± 10 Ma, similar to four zircon fractions analyzed by TIMS that yield a weighted mean of 504 ± 6 Ma (Zhang et al., 2001). The age of the protolith is unconstrained. Further work remains to be done to constrain the cooling and exhumation history.

Discussion

Thermobarometric evidence for UHP metamorphism is preserved at Dulan and the Lüliang Shan in the North Qaidam terrane, and at Bashiwake and Jianggalesayi in the south Altyn terrane (Figs. 6, 9, 12). These P-T estimates are supported by the presence of coesite at Dulan, diamond (and possibly coesite) in the Lüliang Shan, and coesite pseudomorphs at Jianggalesayi. The reasons for disparate P-T estimates from garnet peridotite at Bashiwake are unclear, and so far index minerals such as coesite and diamond have not been identified from this area.

Thermobarometry of garnet peridotite in the Lüliang Shan (Song et al., 2004, 2005) yields a higher pressure and temperature history than the nearby eclogite and metapelite (Fig. 9; Table 1; Zhang et al., 2004a, 2005c). Similarly, thermobarometry of the garnet peridotite near Bashiwake studied by Liu et al. (2002) yields a higher pressure history than the garnet peridotite, metabasite, and felsic gneiss studied by Zhang et al. (2005b). Some mantle-derived ultramafic rocks from UHP terranes may record an older evolution in the deep mantle prior to incorporation in continental host rocks during deep subduction (e.g., Spengler et al., 2006). However, based on mineral chemistry and inclusions, a low-pressure crustal cumulate origin is proposed for peridotite at both Bashiwake and Lüliang Shan (Liu et al., 2002; Song et al., 2004, 2005), rendering an earlier history in the deep mantle unlikely.

Geochronology yields broadly similar metamorphic ages for the five localities (Fig. 14a; Table 2), but the two best studied areas, Dulan and Lüliang Shan, yield a considerable (25–70 m.y.) range in ages interpreted to record eclogite-facies

metamorphism (Fig. 14c; Table 2). The age of eclogite-facies metamorphism may young from west to east (Fig. 14c), but more geochronology from the less extensively studied localities is needed to substantiate this. Intriguingly, at both Dulan and Lüliang Shan, UHP metamorphism appears to be the youngest, at approximately 425 Ma at both localities (Figs. 6, 9). At Dulan, this is preceded by several 10s of m.y. of HP metamorphism, similar to age ranges observed in other UHP terranes: 30–50 m.y. in Northeast Greenland (McClelland et al., 2006), 10–20 m.y. in the Alps and Norway (Lapen et al., 2003; Kylander-Clark et al., 2005), and 20–30 m.y. in the Dabie-Sulu (Leech et al., 2006; Wan et al., 2005). In the Lüliang Shan, HP (±UHP?) metamorphism at 495–488 Ma followed by exhumation at 478–460 Ma is recorded in the northern part of the range (Figs. 4 and 10; Table 2), whereas UHP metamorphism at 420–423 Ma is recorded in ultramafic rocks from the southern Lüliang Shan. As noted above, this young age for UHP metamorphism in the ultramafic rocks appears to conflict with geochronology from the adjacent rocks, and requires further work. Interestingly, the age of UHP metamorphism at ~425 Ma is nearly simultaneous with the change from subduction-related magmatism in the southwest (dioritic to granitic plutons without inherited zircons) to collision-related magmatism in the northeast (granite and leucogranite plutons with common inherited Late Archean–Early Proterozoic zircons), which Gehrels et al. (2003b) suggest is related to accretion-related crustal melting.

Rock associations and protolith ages show strong similarities at the five localities. Pelitic and granitic gneisses host mafic and ultramafic layers and lenses. Magmatic ages for the granitic gneiss at Dulan, Xitie Shan, Lüliang Shan, and Bashiwake are similar, near the Neoproterozoic–Mesoproterozoic boundary (Fig. 14b; Table 2), and isotopic

data from Dulan, Xitie Shan, and Lüliang Shan support a crustal-melt origin for the granites (Mattinson et al., 2006; Menold, unpubl. data; Wan et al., in press; Zhang et al., in review). Inherited detrital zircon grains in paragneiss indicate a significant Mesoproterozoic to Archean contribution at Dulan and Lüliang Shan, and these ages are also present at the less extensively studied Xitie Shan and Bashiwake localities (Figs. 8, 14a). Neodymium model ages also support a Paleoproterozoic source age for the sediments (Wan et al., in press). Similar to many other UHP terranes, the variable composition sedimentary gneisses, quartzite, and marble appears most consistent with an origin as a passive margin sequence. These sediments were subsequently intruded by granites, basaltic dikes and sills, and ultramafic complexes prior to subduction in the Early Paleozoic.

The exhumation history of these rocks will require further thermobarometric and geochronologic constraint. Pressure-temperature paths indicate that some localities, such as Jianggalesayi, northern Lüliang Shan, and possibly the north belt of Dulan record near adiabatic decompression to pressures corresponding to the base of the crust (Figs. 6, 9, and 12). In contrast, the south belt of Dulan records heating during exhumation, and Xitie Shan and Bashiwake also record high temperature conditions (Figs. 6 and 9); it remains to be determined if the latter two localities attained their high temperatures during decompression from lower temperature UHP conditions.

Thermochronologic constraints on exhumation indicate that at Dulan and Lüliang Shan, UHP rocks were exhumed to upper crustal depths within 10–20 m.y., based on muscovite $^{40}Ar/^{39}Ar$ ages (Figs. 7 and 10), which implies minimum exhumation rates of 3–5 mm/a, based on thermobarometry of retrograde mineral assemblages (Menold et al.,

2004; Song et al., 2003b, 2006; Zhang et al., 2005c). In the northwestern part of the Lüliang Shan, exhumation from UHP conditions to upper crustal depths was complete by 460–477 Ma (Menold et al., 2004; Zhang et al., 2005c), but garnet peridotite approximately 40 km southeast was not exhumed until after UHP conditions were attained at 423 Ma, nearly 40 m.y. later (Fig. 10).

Constraints on tectonic models

Any tectonic model for the North Qaidam and South Altyn region must account for HP/UHP metamorphism of continental sediments (likely a passive margin sequence), granites, and minor mafic and crustally-hosted ultramafic rocks for several 10s of m.y. in the Early Paleozoic; the presence of an early Cambrian ophiolite (exposed in the Lüliang Shan); the presence of Early Paleozoic arc-related plutons northeast of the HP/UHP rocks; the presence of Early Paleozoic HP/LT blueschist and eclogite in the North Qilian and North Altyn region, approximately 350 km northeast of the HP/UHP belt; and the presence of cross-cutting granitic plutons intruding the HP/UHP rocks.

Several tectonic models have been proposed to explain some of these observations (Fig. 15). Key differences among the models are the orientation of the subduction zone responsible for HP/UHP metamorphism, and the number of subduction zones responsible for HP/UHP metamorphism, arc magmatism in the Qilian, and HP/LT metamorphism in the North Qilian.

Yin and Harrison (2000) and Yang et al. (2001c, 2002) propose a model involving separate, north-dipping subduction zones for the HP/UHP belt and the HP/LT belt (Fig. 15a, b); Yin and Harrison (2000) also propose a third north-dipping subduction zone to

explain the Danghe Nan Shan suture and arc magmatism in the central Qilian. These models imply that the UHP rocks originated as the northern margin of the basement to the Qaidam basin, and that HP/UHP metamorphism and HP/LT metamorphism occurred in separate, unrelated subduction systems (Fig. 15a, b). Although these models do not explicitly account for the Lüliang Shan ophiolite, it could be generated by forearc extension above the subduction zone responsible for later UHP metamorphism. The presence of multiple sutures implies that Qaidam and South Qilian (and central Qilian as well in the Yin and Harrison (2000) model) were originally separate blocks sutured in the Paleozoic.

Gehrels et al. (2003b) and Sobel and Arnaud (1999) propose a single, south-dipping subduction system in which the slab shallows with time to explain the spatial and temporal distribution of plutons within the Qilian (Fig. 15c-e). In this model, HP/LT rocks of the North Qilian are preserved near the trench between the North China/Tarim craton and the Qilian/central Altyn Tagh (Fig. 15e). Although not explicit in the model, this same subduction zone would also be responsible for UHP metamorphism, and UHP rocks would have originated at the southern margin of the North China/Tarim craton. Metamorphic core complex formation or diapirism would presumably be responsible for final emplacement of the UHP rocks into the Qilian/Qaidam crust, approximately 350 km southwest of the subduction zone. The Qilian and Qaidam originate as a single block in this model (Fig. 15c), in accord with similar-age Proterozoic plutons in both areas suggesting crustal assembly by this time. This model does not account for magmatism northeast of the North Qilian HP/LT belt, or the Lüliang Shan ophiolite, which presumably would have formed as a small, Sea of Japan-type back-arc basin.

Song et al. (2006) propose a single, north-dipping subduction system to account for HP/LT metamorphism in the North Qilian and HP/UHP metamorphism in the North Qaidam (Fig. 15f-h). This model implies that the UHP rocks originated as the northern margin of the basement to the Qilian/Qaidam block (Fig. 15f), and that HP eclogite formed at ~460 Ma, originated as oceanic crust, and was tectonically emplaced within the continental, UHP slab at ~420 Ma. The UHP rocks reached their present location by ~350 km of subhorizontal exhumation through the central Qilian lithosphere (Fig. 15h). This model does not account for Paleozoic magmatism within the Qilian, or the Lüliang Shan ophiolite. More extensive regional geologic mapping and geochronology is needed to better constrain the tectonic models for this area.

The distinctive HP/UHP metamorphism, age, and rock association has been proposed as a piercing line to constrain total offset on the Altyn Tagh fault (Fig. 1), and yields estimates of 350–400 km (Yang et al., 2001c; Zhang et al., 2001, 2005b, 2005c). These estimates are consistent with constraints derived from other offset tectonic belts (Yue and Liou, 1999; Cowgill et al., 2003), offset plutonic belts (Gehrels et al., 2003b), offset Jurassic facies boundaries (Ritts and Biffi, 2001), and offset Cenozoic basins (Yue et al., 2001).

The similarity of age, metamorphic conditions, and rock associations in the Qaidam–Qilian–Altyn areas documented in this review supports correlation of these localities, but existing work leaves several key tectonic questions unanswered. Determining the number and polarity of subduction zones responsible for HP/UHP metamorphism, arc magmatism, and assembly of arcs and/or continental fragments is essential to discriminate among the possible tectonic models of the Qaidam–Qilian–Altyn

areas. Investigating the westward extension of the South Altyn terrane and the southeastern extension of the North Qaidam terrane, and its relationship with the west Qinling terrane will provide critical constraints on tectonic models. Geologic mapping both within the HP/UHP terranes as well as in areas to the east (Fig. 1) will be necessary to address these problems. Research targets with the HP/UHP terranes include investigation of the HP/UHP and exhumation history, especially geographic variation in exhumation processes and timing, investigation of a possible earlier, UHP history at Xitie Shan and Bashiwake, and constraining the relationship between the garnet peridotite in the southern Lüliang Shan and the adjacent rocks. We expect that continued investigation will result in an improved understanding of the paleogeographic evolution of western China, as well as significantly advance our understanding of continental growth and modification at convergent margins.

Acknowledgements

We submit this paper in honor of Prof. J.G. "Louie" Liou's retirement from Stanford and his many accomplishments in the field of high- and ultra-high pressure metamorphism. We thank George Gehrels and Mary Leech for helpful reviews. C.G.M. thanks A. Bian and S.Y. Chen for assistance in the field, F.K. Mazdab, B. Wiegand, J.R. Metcalf, T. Tsujimori, and M. Vogel for assistance with the SHRIMP-RG analyses, and C.A.M. thanks A. Yin and C. Manning. This research was supported by grants from Stanford University, the Geological Society of America (Grant #7466-03), the National Science Foundation (NSF-EAR0408690 and NSF-EARXXXXXXX), and the National Science Foundation of China (Grant # 40272095 and 40472102).

References

Bureau of Geology and Mineral Resources of Qinghai Province (BGMQ), 1991, Regional Geology of Qinghai Province, Geological Memoirs: Beijing, Geological Publishing House, 662 p. (in Chinese with English abstract).

Bureau of Geology and Mineral Resources of Xinjiang Uygur Autonomous Region (BGMX), 1993, Regional Geology of Xinjiang Uygur Autonomous Region, Geological Memoirs: Beijing, Geological Publishing House, 841 p. (in Chinese with English abstract).

Chopin, C., 1984, Coesite and pure pyrope in high-grade blueschists of the western Alps: a first record and some consequences: Contributions to Mineralogy and Petrology, v. 86, p. 107-118.

Chu, C.-Y., 1998, Eclogites in the Altun Mountains, SE Tarim, NW China [MS thesis]: Stanford University, 78 p.

Coleman, R. G., and Wang, X., 1995, Overview of the geology and tectonics of UHPM, in Coleman, R. G., and Wang, X., eds., Ultrahigh Pressure Metamorphism: New York, Cambridge University Press, p. 1-32.

Cowgill, E., Yin, A., Harrison, T. M., and Xiao-Feng, W., 2003, Reconstruction of the Altyn Tagh fault based on U-Pb geochronology: Role of back thrusts, mantle sutures, and heterogeneous crustal strength in forming the Tibetan Plateau: Journal of Geophysical Research, v. 108, no. B7, p. 2346, doi:10.1029/2002JB002080.

Ernst, W. G., and Liou, J. G., 2000, Overview of UHP metamorphism and tectonics in well-studied collisional orogens, in Ernst, W. G., and Liou, J. G., eds., Ultra-High Pressure

Metamorphism and Geodynamics in Collision-Type Orogenic Belts: Columbia, Maryland, Bellwether Publishing, p. 3-19.

Gehrels, G. E., Yin, A., and Wang, X.-F., 2003a, Detrital-zircon geochronology of the northeastern Tibetan plateau: Geological Society of America Bulletin, v. 115, no. 7, p. 881-896.

-, 2003b, Magmatic history of the northeastern Tibetan Plateau: Journal of Geophysical Research, v. 108, no. B9, p. 2423, doi:10.1029/2002JB001876.

Hanson, A., Chang, E., Zhou, D., Ritts, B., Sobel, E., Graham, S., Chu, C., Liu, J., Zhang, R. Y., and Liou, J. G., 1995, Discovery of eclogite blocks in the Altun Mountains, SE Tarim basin, NW China: Eos Transactions, AGU, v. 76, p. S283.

Holland, T. J. B., and Powell, R., 1998, An internally consistent thermodynamic data set for phases of petrological interest: Journal of Metamorphic Geology, v. 16, p. 309-343.

Kretz, R., 1983, Symbols for rock-forming minerals: American Mineralogist, v. 68, p. 277-279.

Kusky, T. M., and Li, J., 2003, Paleoproterozoic tectonic evolution of the North China Craton: Journal of Asian Earth Sciences, v. 22, no. 4, p. 383-397.

Kylander-Clark, A., Hacker, B., Johnson, C., Beard, B., Mahlen, N., and Lapen, T., 2005, Lu/Hf and Sm/Nd ages of eclogite-facies metamorphism in the Western Gneiss Region, Norway: Geological Society of America Abstracts with Programs, v. 37, no. 7, p. 390.

Lapen, T. J., Johnson, C. M., Baumgartner, L. P., Mahlen, N. J., Beard, B. L., and Amato, J. M., 2003, Burial rates during prograde metamorphism of an ultra-high-pressure terrane: an example from Lago di Cignana, western Alps, Italy: Earth and Planetary Science Letters, v. 215, p. 57-72.

Leech, M. L., Webb, L. E., and Yang, T. N., 2006, Diachronous histories for the Dabie-Sulu orogen from high-temperature geochronology, in Hacker, B. R., McClelland, W. C., and Liou, J. G., eds., Geological Society of America Special Paper 403, Ultrahigh-pressure metamorphism: Deep continental subduction, Geological Society of America, p. 1-22.

Li, H. K., Lu, S. N., Zhao, F. Q., and Yu, H. F., 1999, Determination and significance of the coesite eclogite on the Yuqia river on the north margin of the Qaidam basin: Geoscience, v. 13, p. 43-50 (Chinese with English abstract).

Liou, J. G., Zhang, R. Y., Katayama, I., and Maruyama, S., 2002, Global distribution and petrotectonic characterizations of UHPM terranes, in Parkinson, C. D., Katayama, I., Liou, J. G., and Maruyama, S., eds., The diamond-bearing Kokchetav massif, Kazakhstan: Tokyo, Japan, Universal Academy Press, p. 15-35.

Lu, S. N., 2003, Preliminary study of Precambrian geology in the North Tibet--Qinghai Plateau: Beijing, China, Geological Publishing House, 125 p.

Mattinson, C. G., Liou, J. G., Bird, D. K., Wooden, J. L., Wu, C., and Yang, J., 2005, Zircon geochronology and REE geochemistry, North Qaidam UHP terrane, northwest China: Mitteilungen der Österreichischen Mineralogischen Gesellschaft, v. 150, p. 106.

Mattinson, C. G., Liou, J. G., Jones, R. E., Wooden, J. L., Wu, C. L., and Yang, J. S., 2003, Exsolution textures and zircon geochemistry, North Qaidam UHP terrane, NW China: Eos Transactions, AGU, v. 84, no. 46, p. F1532.

Mattinson, C. G., Wooden, J. L., Liou, J. G., Bird, D. K., and Wu, C. L., 2006, Geochronology and tectonic significance of Middle Proterozoic granitic orthogneiss, North Qaidam HP/UHP terrane, Western China: Mineralogy and Petrology, v. 88, p. 227-241.

-, in press, Age and duration of eclogite-facies metamorphism, North Qaidam HP/UHP terrane, western China: American Journal of Science.

McClelland, W. C., Power, S. a. E., Gilotti, J. A., Mazdab, F. K., and Wopenka, B., 2006, U-Pb SHRIMP geochronology and trace element geochemistry of coesite-bearing zircons, North-East Greenland Caledonides, in Hacker, B. R., McClelland, B., and Liou, J. G., eds., Geological Society of America Special Paper 403, Ultrahigh-Pressure Metamorphism: Deep Continental Subduction, Geological Society of America, p. 23-43.

Menold, C. A., Manning, C. E., Yin, A., and Chen, X., 2004, Geology of the North Qaidam HP-UHP terrane, Western China: Eos Transactions, AGU, v. 85, no. 47, p. F1679.

Poli, S., and Schmidt, M. W., 1995, H_2O transport and release in subduction zones: Experimental constraints on basaltic and andesitic systems: Journal of Geophysical Research, v. 100, no. B11, p. 22299-22314.

Ritts, B. D., and Biffi, U., 2000, Magnitude of post-Middle Jurassic (Bajocian) displacement on the central Altyn Tagh fault system, northwest China: Geological Society of America Bulletin, v. 112, no. 1, p. 61-74.

Rubatto, D., 2002, Zircon trace element geochemistry: partitioning with garnet and the link between U-Pb ages and metamorphism: Chemical Geology, v. 184, p. 123-138.

Smith, D. C., 1984, Coesite in clinopyroxene in the Caledonides and its implications for geodynamics: Nature, v. 310, p. 641-644.

Sobel, E. R., and Arnaud, N., 1999, A possible middle Paleozoic suture in the Altyn Tagh, NW China: Tectonics, v. 18, no. 1, p. 64-74.

Sobolev, N. V., and Shatsky, V. S., 1990, Diamond inclusions in garnets from metamorphic rocks: a new environment for diamond formation: Nature, v. 343, p. 742-746.

Song, S., Yang, J., Liou, J. G., Wu, C., Shi, R., and Xu, Z., 2003, Petrology, geochemistry and isotopic ages of eclogites from the Dulan UHPM terrane, the North Qaidam, NW China: Lithos, v. 70, p. 195-211.

Song, S., Zhang, L., and Niu, Y., 2004, Ultra-deep origin of garnet peridotite from the North Qaidam ultrahigh-pressure belt, Northern Tibetan Plateau, NW China: American Mineralogist, v. 89, p. 1330-1336.

Song, S., Zhang, L., Niu, Y., Li, S., Song, B., and Liu, D., 2006, Evolution from oceanic subduction to continental collision: a case study from the northern Tibetan Plateau based on geochemical and geochronological data: Journal of Petrology, v. 47, no. 3, p. 435-455.

Song, S., Zhang, L., Niu, Y., Su, L., Jian, P., and Liu, D., 2005, Geochronology of diamond-bearing zircons from garnet peridotite in the North Qaidam UHPM belt, Northern Tibetan Plateau: A record of complex histories from oceanic lithosphere subduction to continental collision: Earth and Planetary Science Letters, v. 234, p. 99-118.

Song, S. G., Yang, J. S., Xu, Z. Q., Liou, J. G., and Shi, R. D., 2003, Metamorphic evolution of the coesite-bearing ultrahigh-pressure terrane in the North Qaidam, Northern Tibet, NW China: Journal of Metamorphic Geology, v. 21, p. 631-644.

Spengler, D., van Roermund, H. L. M., Drury, M. R., Ottolini, L., Mason, P. R. D., and Davies, G. R., 2006, Deep origin and hot melting of an Archaean orogenic peridotite massif in Norway: Nature, v. 440, no. 7086, p. 913-917.

Wan, Y., Li, R., Wilde, S. A., Liu, D., Chen, Z., Yan, L., Song, T., and Yin, X., 2005, UHP metamorphism and exhumation of the Dabie Orogen, China: Evidence from SHRIMP dating of zircon and monazite from a UHP granitic gneiss cobble from the Hefei Basin: Geochimica et Cosmochimica Acta, v. 69, no. 17, p. 4333-4348.

Wan, Y., Zhang, J., Yang, J., and Xu, Z., 2006, Geochemistry of high-grade metamorphic rocks of the North Qaidam mountains and their geological significance: Journal of Asian Earth Sciences, p. in press.

Wan, Y. S., Xu, Z. Q., Yang, J. S., and Zhang, J. X., 2001, Ages and compositions of the Precambrian high-grade basement of the Qilian Terrane and its adjacent areas: Acta Geologica Sinica, v. 75, p. 375-384.

Wang, E., and Burchfiel, B. C., 2004, Late Cenozoic right-lateral movement along the Wenquan fault and associated deformation: Implications for the kinematic history of the Qaidam Basin, northeastern Tibetan Plateau: International Geology Review, v. 46, p. 861-879.

Wu, C., Yang, J., Wooden, J., Ernst, W. G., Liou, J. G., Li, H., Zhang, J., Wan, Y., and Shi, R., 2001, Relationship between UHP eclogite and two different types of granite in the North Qaidam, NW China: Evidence from zircon SHRIMP ages of granites: Eos Transactions, AGU, v. 82, no. 47, p. Abstract V32C-0980.

Wu, C., Yang, J., Wooden, J., Liou, J. G., Li, H., Shi, R., Meng, F., Persing, H., and Meibom, A., 2002, Zircon SHRIMP dating of granite from Qaidamshan, NW China: Chinese Science Bulletin, v. 47, no. 5, p. 418-422.

Wu, C., Yang, J., Wooden, J. L., Shi, R., Chen, S., Meibom, A., and Mattinson, C., 2004, Zircon U-Pb SHRIMP dating of the Yematan Batholith in Dulan, north Qaidam, NW China: Chinese Science Bulletin, v. 49, no. 16, p. 1736-1740.

Yang, J., Liu, F., Wu, C., Xu, Z., Shi, R., and Chen, S., 2005, Two ultrahigh-pressure metamorphic events recognized in the Central Orogenic Belt of China: Evidence from the U-Pb dating of coesite-bearing zircons: International Geology Review, v. 47, p. 327-343.

Yang, J., Song, S., Xu, Z., Wu, C., Mattinson, C., Bian, A., Zhang, R. Y., Liou, J. G., and Ernst, W. G., 2001a, Northern Qaidam Caledonian UHP terrane: A new discovery: Eos Transactions, AGU, v. 82, no. 47, p. F1342.

Yang, J., Wu, C., Zhang, J., Song, S., and Ireland, T. R., 2001b, U-Pb/Sm-Nd/Ar-Ar ages of the North Qaidam ultrahigh-high pressure metamorphic rocks, NW China, in Sixth International Eclogite Conference, Niihama, Japan, p. 178.

Yang, J., Xu, Z., Song, S., Wu, C., Shi, R., Zhang, J., Wan, Y., Li, H., Jin, X., and Jolivet, M., 2000, Discovery of eclogite in Dulan, Qinghai Province and its significance for studying the HP--UHP metamorphic belt along the Central Orogenic Belt of China: Acta Geologica Sinica, v. 74, no. 2, p. 156-168.

Yang, J., Xu, Z., Zhang, J., Chu, C.-Y., Zhang, R., and Liou, J.-G., 2001c, Tectonic significance of Early Paleozoic high-pressure rocks in Altun--Qaidam--Qilian Mountains, NW China: Geological Society of America Memoir, v. 194, p. 151-170.

Yang, J., Xu, Z., Zhang, J., Song, S., Wu, C., Shi, R., Li, H., and Brunel, M., 2002, Early Paleozoic North Qaidam UHP metamorphic belt on the north-eastern Tibetan plateau and a paired subduction model: Terra Nova, v. 14, no. 5, p. 397-404.

Yang, J. J., Zhu, H., Deng, J. F., Zhou, T. Z., and Lai, S. C., 1994, Discovery of garnet-peridotite at the northern margin of the Qaidam basin and its significance: Acta Petrologica et Mineralogica, v. 13, no. 2, p. 97-105 (in Chinese with English abstract).

Yang, J. S., Xu, Z. Q., Li, H. B., Wu, C. L., Cui, J. W., Zhang, J. X., and Chen, W., 1998, Discovery of eclogite at northern margin of Qaidam basin, NW China: Chinese Science Bulletin, v. 43, p. 1755-1760 (in Chinese with English abstract).

Yin, A., and Harrison, T. M., 2000, Geologic evolution of the Himalayan-Tibetan orogen: Annual Review of Earth and Planetary Sciences, v. 28, p. 211-280.

Yue, Y., and Liou, J. G., 1999, Two-stage evolution model for the Altyn Tagh fault, China: Geology, v. 27, no. 3, p. 227-230.

Yue, Y., Ritts, B. D., and Graham, S. A., 2001, Initiation and long-term slip history of the Altyn Tagh fault: International Geology Review, v. 43, p. 1087-1093.

Zhang, J., Mattinson, C. G., Meng, F., Wan, Y., and Dong, K., in review, Polyphase tectonothermal history recorded in granulitized gneisses from the North Qaidam HP/UHP metamorphic terrane, Western China: evidence from zircon U-Pb geochronology: Geological Society of America Bulletin.

Zhang, J., Meng, F., and Yang, J., 2005a, A new HP/LT metamorphic terrane in the northern Altyn Tagh, western China: International Geology Review, v. 47, p. 371-386.

Zhang, J., Yang, J., Meng, F., Wan, Y., Li, H., and Wu, C., in press, U-Pb isotopic studies of eclogites and their host gneisses in the Xitieshan area of the North Qaidam mountains, western China: New evidence for an early Paleozoic HP-UHP metamorphic belt: Journal of Asian Earth Sciences.

Zhang, J., Zhang, Z., Xu, Z., Yang, J., and Cui, J., 2001, Petrology and geochronology of eclogites from the western segment of the Altyn Tagh, northwestern China: Lithos, v. 56, p. 187-206.

Zhang, J. X., Mattinson, C. G., Meng, F. C., and Wan, Y. S., 2005b, An Early Palaeozoic HP/HT granulite-garnet peridotite association in the south Altyn Tagh, NW China: P-T history and U-Pb geochronology: Journal of Metamorphic Geology, v. 23, no. 7, p. 491-510.

Zhang, J. X., Meng, F. C., and Yang, J. S., 2004a, Eclogitic metapelites in the western segment of the north Qaidam Mountains: Evidence on “in situ” relationship between eclogite and its country rocks: Science in China, Series D, Earth Sciences, v. 12, p. 1102-1112.

Zhang, J. X., Yang, J. S., Mattinson, C. G., Xu, Z. Q., Meng, F. C., and Shi, R. D., 2005c, Two contrasting eclogite cooling histories, North Qaidam HP/UHP terrane, western China: Petrological and isotopic constraints: Lithos, v. 84, no. 1-2, p. 51-76.

Zhang, J. X., Yang, J. S., Xu, Z. Q., Meng, F. C., Li, H. B., and Shi, R. D., 2002, Evidence for UHP metamorphism of eclogites from the Altun Mountains: Chinese Science Bulletin, v. 47, no. 9, p. 751-755.

Zhang, R. Y., Liou, J. G., Yang, J. S., Liu, L., and Jahn, B.-m., 2004b, Garnet peridotites in UHP mountain belts of China: International Geology Review, v. 46, p. 981-1004.

Zheng, J., Griffin, W. L., O'Reilly, S. Y., Zhang, M., Pearson, N., and Pan, Y., 2006, Widespread Archean basement beneath the Yangtze craton: Geology, v. 34, no. 6, p. 417-420.

Figure Captions

Fig. 1. (a) Map of China showing the location of this study (box) and the trends of major mountain belts (dashed lines). (b) Schematic map of the Qaidam-Qilian-Altyn Tagh region showing major tectonic units, and locations of eclogite and garnet peridotite. The

boxes indicate the locations of Figs. 2–4. Ages of Proterozoic (meta)granites are referenced in Table 2. The Wenquan fault is located in the southeast corner of the map, between the North Qaidam terrane and the Gonghe Basin. Modified from Zhang et al. (2005b).

Fig. 2. Geologic map of the Dulan area showing sample locations. The town of Dulan is approximately 30 km southwest of map area. Modified from Yang et al. (2000), Wu et al. (2004), and mapping by C.G. Mattinson.

Fig. 3. Geologic map of the Xitie Shan area showing sample locations. The town of Xitie Shan is approximately 5 km south of map area. Modified from Zhang et al. (2005c).

Fig. 4. Geologic map of the Lüliang Shan area showing sample locations. Based on mapping by C.A. Menold.

Fig. 5. (a) Mafic and ultramafic layers in gneiss, North belt, view to the north. (b) Yematan granite truncates foliation in Dakendaban gneiss. (c) Thin section of typical coarse-grained eclogite. (d) Strongly serpentinized garnet peridotite; garnet is largely replaced by spinel. Plane polarized light. (e) Chlorite clinopyroxenite, plane polarized light. Clinopyroxene porphyroblasts contain oriented rods and plates of Cr-magnetite and Cr-chlorite. Note that inclusion-free porphyroblast rims and matrix clinopyroxene contact Cr-chlorite on straight grain boundaries.

Fig. 6. Summary of thermobarometry from the Dulan area (Song et al., 2003b). Polymorphic transitions calculated from Holland and Powell (1998).

Fig. 7. Summary of metamorphic geochronology from the Dulan area. Height of bars represents 2σ uncertainty, and grey bands indicate age ranges associated with the labeled events. References: 1, Song et al., 2003a; 2, Lu, 2003; 3, Song et al., 2006; 4, Mattinson et al., in press; 5, Yang et al., 2005; 6, Mattinson et al., 2005.

Fig. 8. Relative probability plot of zircon core ages from Dulan paragneiss samples. Probability peaks are similar to North China Craton age peaks (grey bands).

Fig. 9. Summary of thermobarometry from the Xitie Shan and Lüliang Shan areas. Polymorphic transitions calculated from Holland and Powell (1998). References: 1, Zhang et al., 2005c (Lüliang Shan eclogite hatched, Xitie Shan eclogite unpatterened); 2, Zhang et al., 2004a (metapelite, fine stipple); 3, C.A. Menold, unpubl. data (eclogite, unpatterened); 4, Song et al., 2004, 2005 (stipple); 5, Zhang et al., 2004b (sparse stipple).

Fig. 10. Summary of geochronology from the Xitie Shan and Lüliang Shan areas. Height of bars represents 2σ uncertainty, except for bars labeled "age range", which represents the range of multiple analyses. Grey bands indicate age ranges associated with the labeled events . References: 1, Menold et al., 2004; 2, Zhang et al., 2000; 3, Zhang et al., 2005c; 4, Song et al., 2005; 5, Zhang et al., in press.

Fig. 11. Bashiwake felsic granulite enclosing garnet peridotite (a) and mafic granulite (b, c, d). Field of view in (a) and (b) is approximately 50 m.

Fig. 12. Summary of thermobarometry from the Bashiwake and Jianggalesayi areas. Polymorphic transitions calculated from Holland and Powell (1998). References: 1, Zhang et al., 2001, 2002; 2, Zhang et al., 2005b; 3, Liu et al., 2002.

Fig. 13. Summary of geochronology from the Bashiwake and Jianggalesayi areas. Height of bars represents 2σ uncertainty. Data for Bashiwake from Zhang et al. (2005b), and data from Jianggalesayi from Zhang et al. (2001).

Fig. 14. Summary of zircon geochronology from the South Altyn and North Qaidam localities. (a) Ages of paragneiss detrital cores, granitic orthogneiss, and ages interpreted to reflect high-pressure metamorphism. Height of bars represents the age range of multiple analyses. (b) Ages of granitic orthogneiss samples, interpreted to reflect magmatic crystallization. Height of bars represents 2σ uncertainty. (c) Ages interpreted to reflect high-pressure metamorphism. Black bars represent range of weighted mean ages, grey bars represent the range of 2σ uncertainty. Individual analyses outside the main group of analyses are plotted separately for Lüliang Shan, Xitie Shan, and Dulan. References: 1, C.G. Mattinson, unpubl. data; 2, Wan et al., 2001; 3, Gehrels et al., 2003b; 4, Zhang et al., in press; 5, Mattinson et al., 2006.

Fig. 15. Summary of proposed tectonic models. (a-b) Model of Yin and Harrison, 2000, Yang et al., 2001c; (c-e) Model of Gehrels et al., 2003b; (f-h) Model of Song et al., 2006.

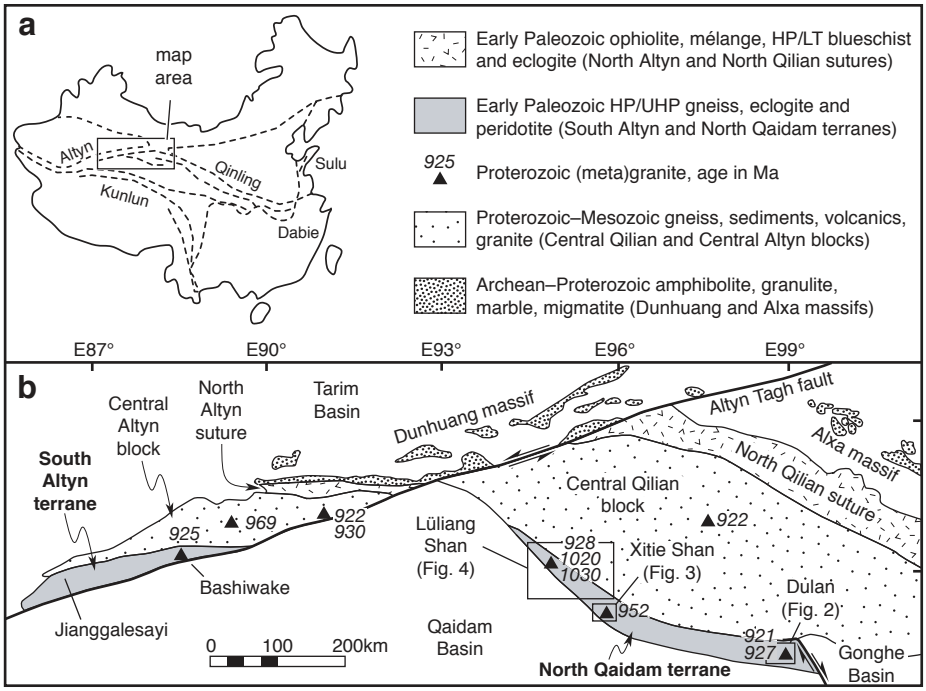
a
map area
Altyn
Qinling
Kunlun
Sulu
Dabie
Early Paleozoic ophiolite, mélange, HP/LT blueschist and eclogite (North Altyn and North Qilian sutures)
Early Paleozoic HP/UHP gneiss, eclogite and peridotite (South Altyn and North Qaidam terranes)
925
Proterozoic (meta)granite, age in Ma
Proterozoic–Mesozoic gneiss, sediments, volcanics, granite (Central Qilian and Central Altyn blocks)
Archean–Proterozoic amphibolite, granulite, marble, migmatite (Dunhuang and Alxa massifs)
E87°
E90°
E93°
E96°
E99°
b
Central Altyn block
North Altyn suture
Tarim Basin
Dunhuang massif
Altyn Tagh fault
Alxa massif
N40°
South Altyn terrane
925
969
922
930
Central Qilian block
922
North Qilian suture
Lüliang Shan (Fig. 4)
928
1020
1030
Xitie Shan (Fig. 3)
N38°
Bashiwake
Jianggalesayi
0 100 200km
Qaidam Basin
952
Dulan (Fig. 2)
921
927
Gonghe Basin
North Qaidam terrane

Fig. 1

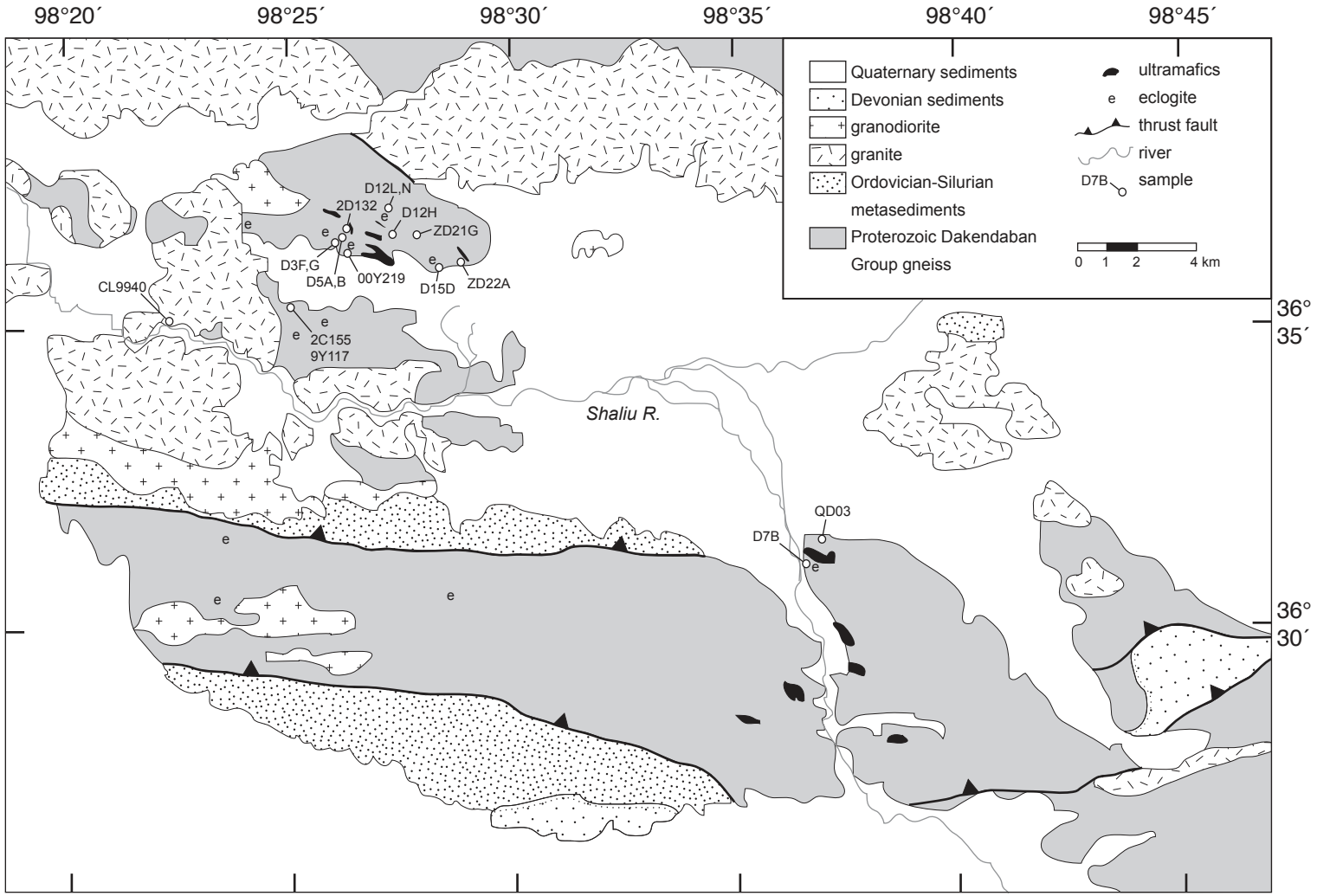
98°20´
98°25´
98°30´
98°35´
98°40´
98°45´
36° 35´
36° 30´
Quaternary sediments
Devonian sediments
granodiorite
granite
Ordovician-Silurian metasediments
Proterozoic Dakendaban Group gneiss
ultramafics
eclogite
thrust fault
river
sample
0 1 2 4 km
D12L,N
2D132
D12H
ZD21G
D3F,G
D5A,B
00Y219
D15D
ZD22A
CL9940
2C155
9Y117
Shaliu R.
QD03
D7B

Fig. 2

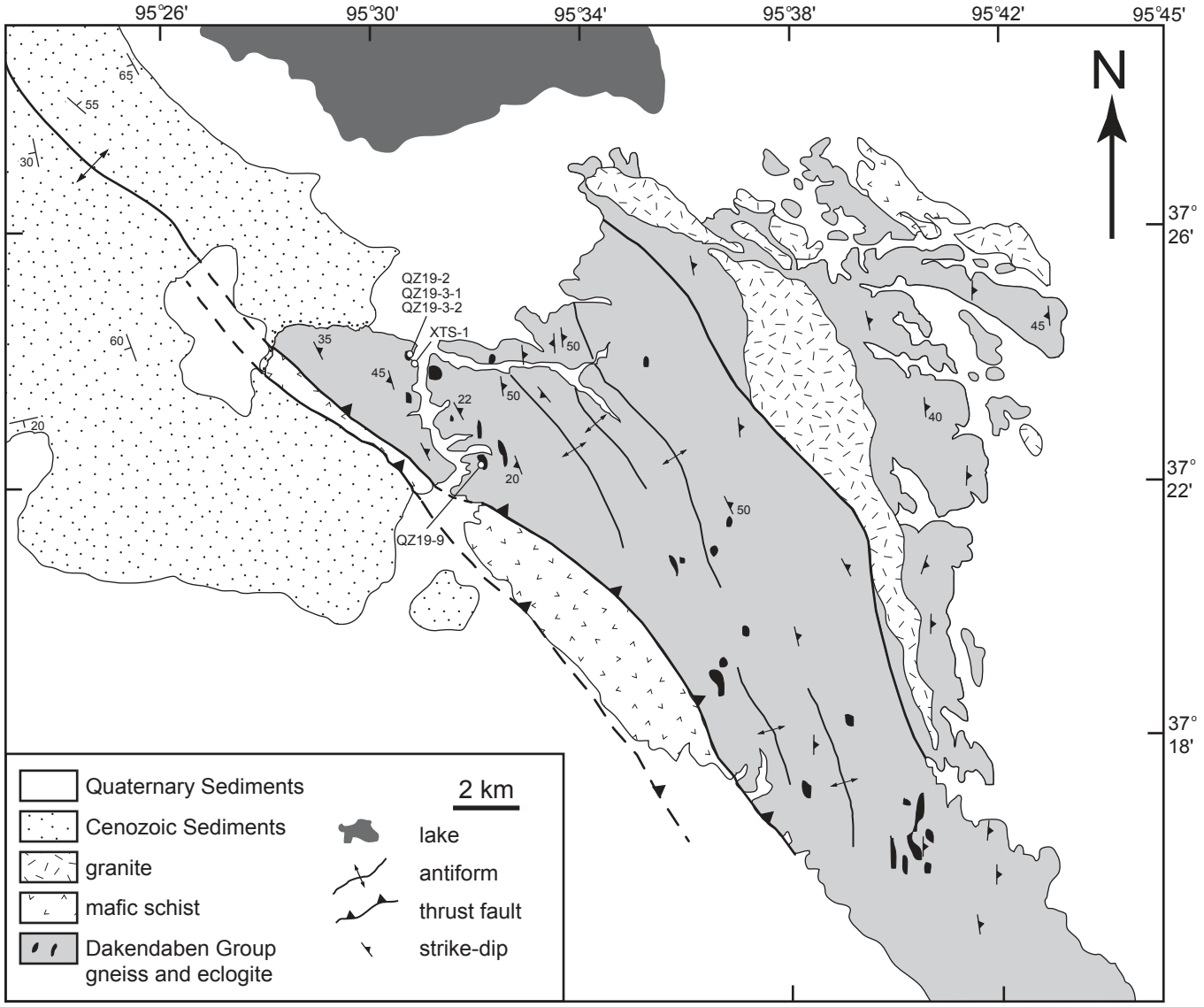
95°26'
95°30'
95°34'
95°38'
95°42'
95°45'
N
37° 26'
37° 22'
37° 18'
QZ19-2
QZ19-3-1
QZ19-3-2
XTS-1
QZ19-9
65
55
30
60
20
35
45
22
50
20
50
45
40
Quaternary Sediments
Cenozoic Sediments
granite
mafic schist
Dakendaben Group gneiss and eclogite
2 km
lake
antiform
thrust fault
strike-dip

Fig. 3

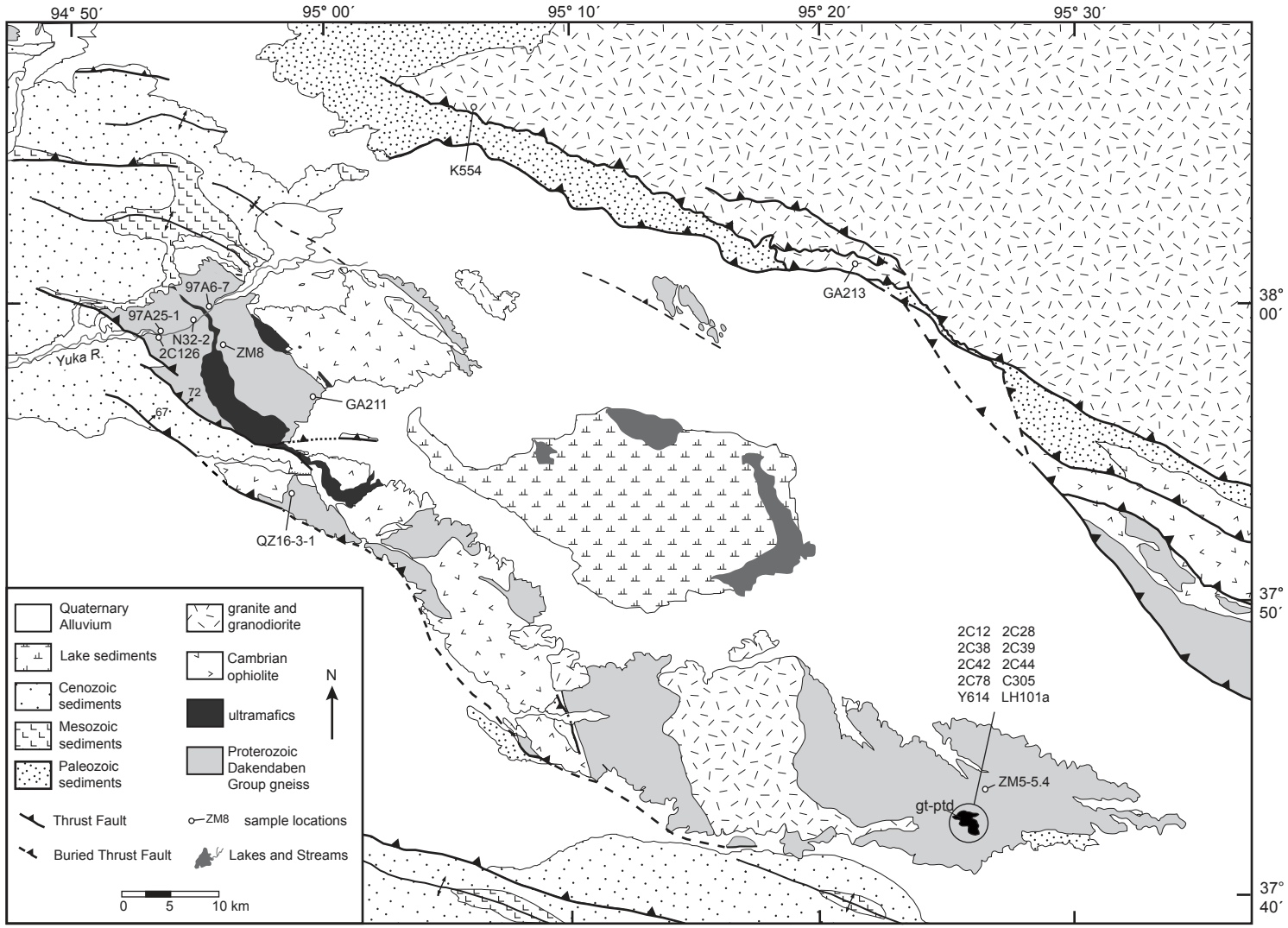
94° 50´
95° 00´
95° 10´
95° 20´
95° 30´
38° 00´
37° 50´
37° 40´
K554
GA213
97A6-7
97A25-1
N32-2
2C126
ZM8
Yuka R.
72
67
GA211
QZ16-3-1
2C12 2C28
2C38 2C39
2C42 2C44
2C78 C305
Y614 LH101a
ZM5-5.4
gt-ptd
Quaternary Alluvium
Lake sediments
Cenozoic sediments
Mesozoic sediments
Paleozoic sediments
granite and granodiorite
Cambrian ophiolite
ultramafics
Proterozoic Dakendaben Group gneiss
N
Thrust Fault
Buried Thrust Fault
ZM8 sample locations
Lakes and Streams
0 5 10 km

Fig. 4

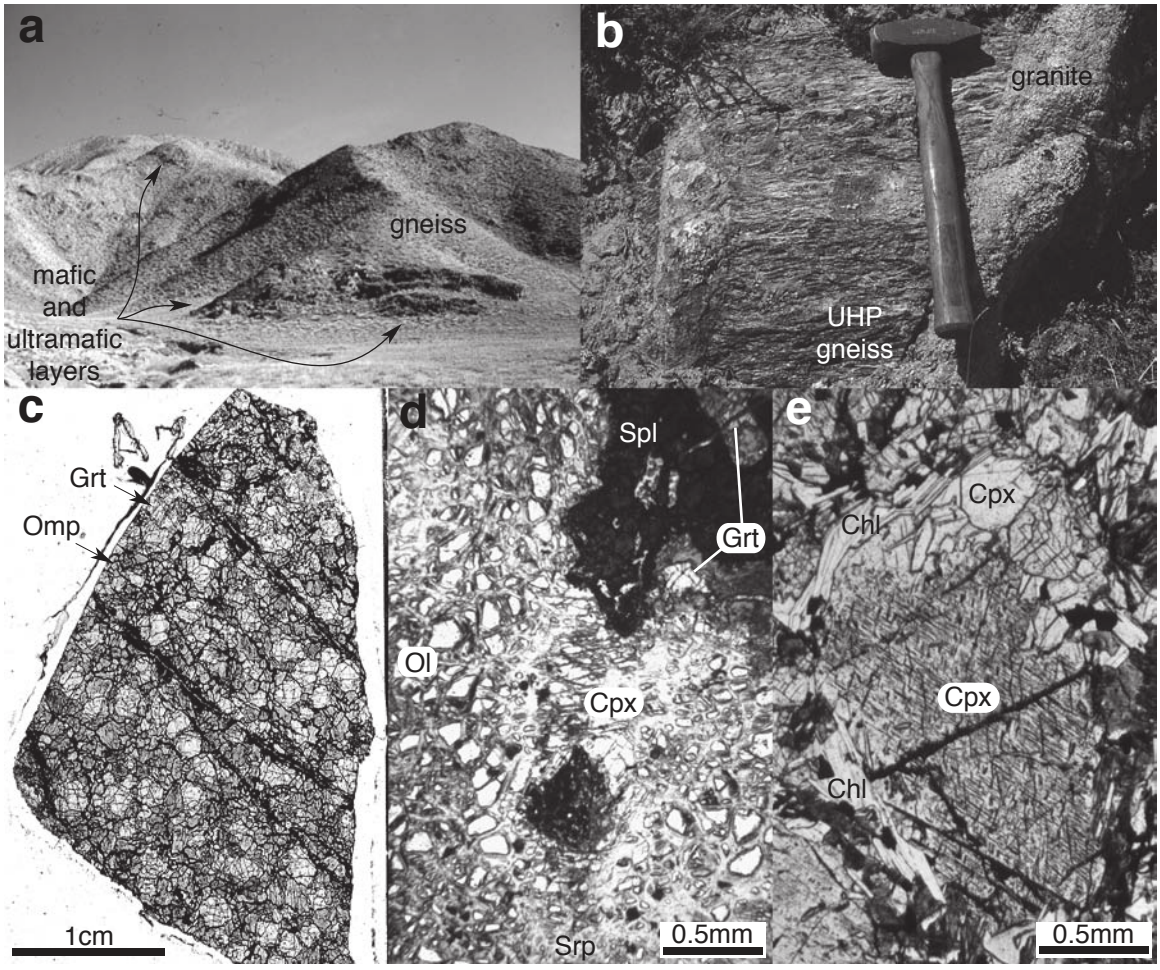
a
gneiss
mafic
and
ultramafic
layers
b
granite
UHP
gneiss
c
Grt
Omp
1cm
d
Spl
Grt
Ol
Cpx
Srp
0.5mm
e
Cpx
Chl
Cpx
Chl
0.5mm

Fig. 5

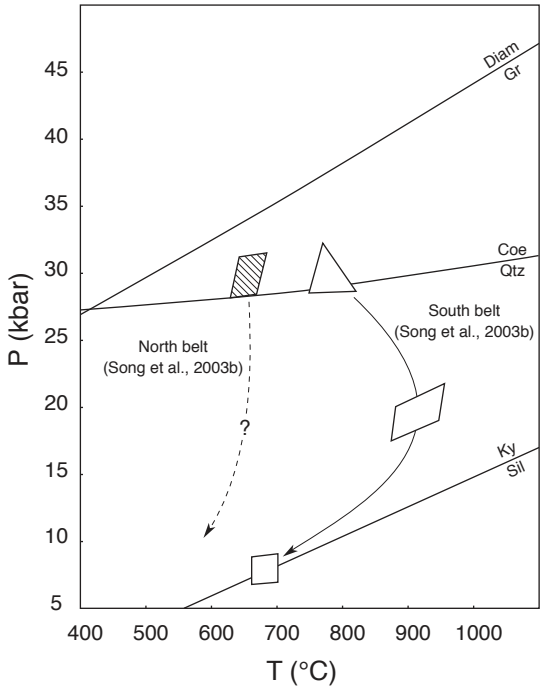
Diam
Gr
Coe
Qtz
South belt
(Song et al., 2003b)
North belt
(Song et al., 2003b)
?
Ky
Sil
P (kbar)
T (°C)
45
40
35
30
25
20
15
10
5
400
500
600
700
800
900
1000

Fig. 6

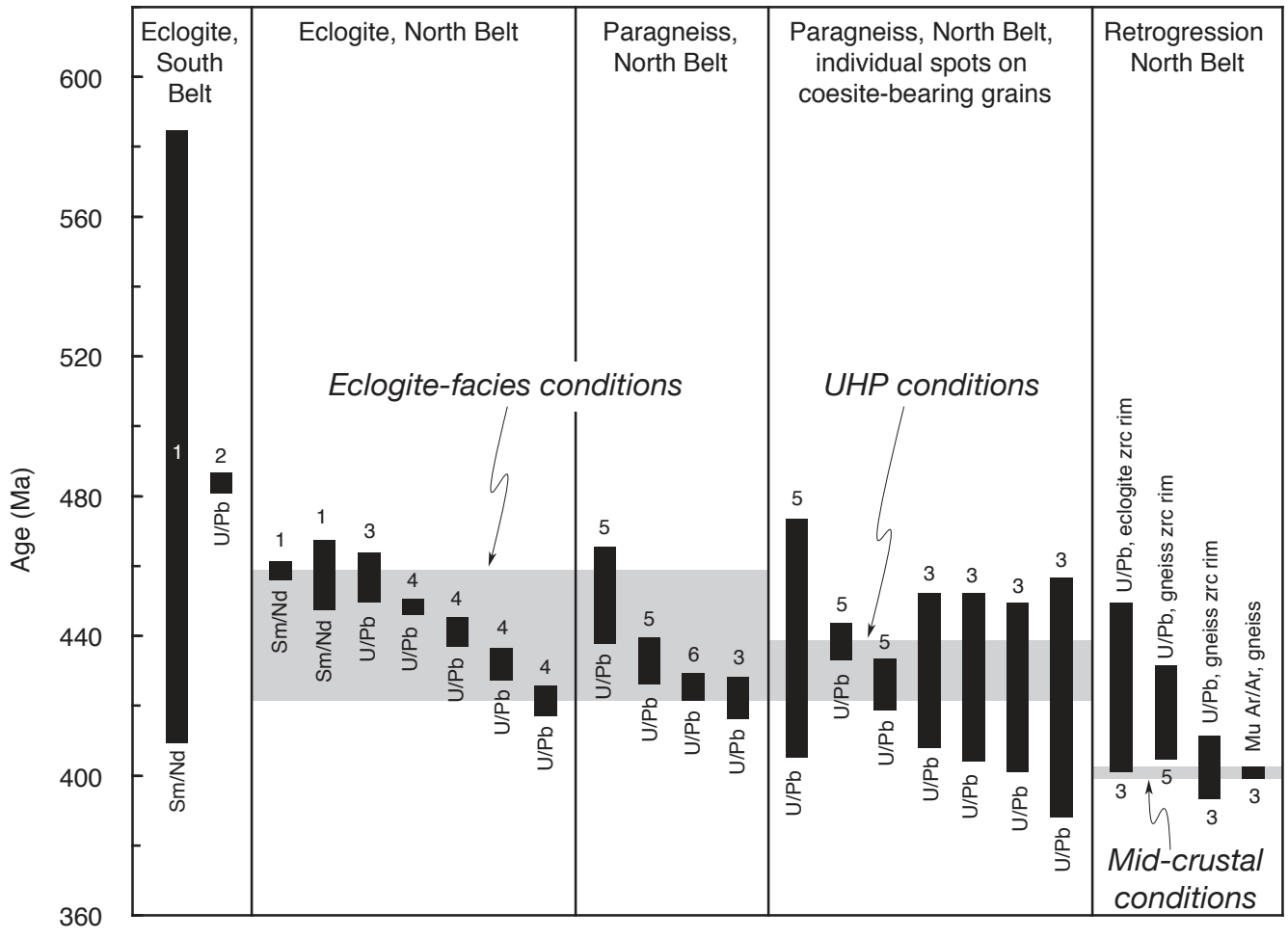
Eclogite, South Belt
Eclogite, North Belt
Paragneiss, North Belt
Paragneiss, North Belt, individual spots on coesite-bearing grains
Retrogression North Belt
Age (Ma)
600
560
520
480
440
400
360
Eclogite-facies conditions
UHP conditions
Mid-crustal conditions
Sm/Nd
U/Pb
U/Pb, eclogite zrc rim
U/Pb, gneiss zrc rim
U/Pb, gneiss zrc rim
Mu Ar/Ar, gneiss

Fig. 7

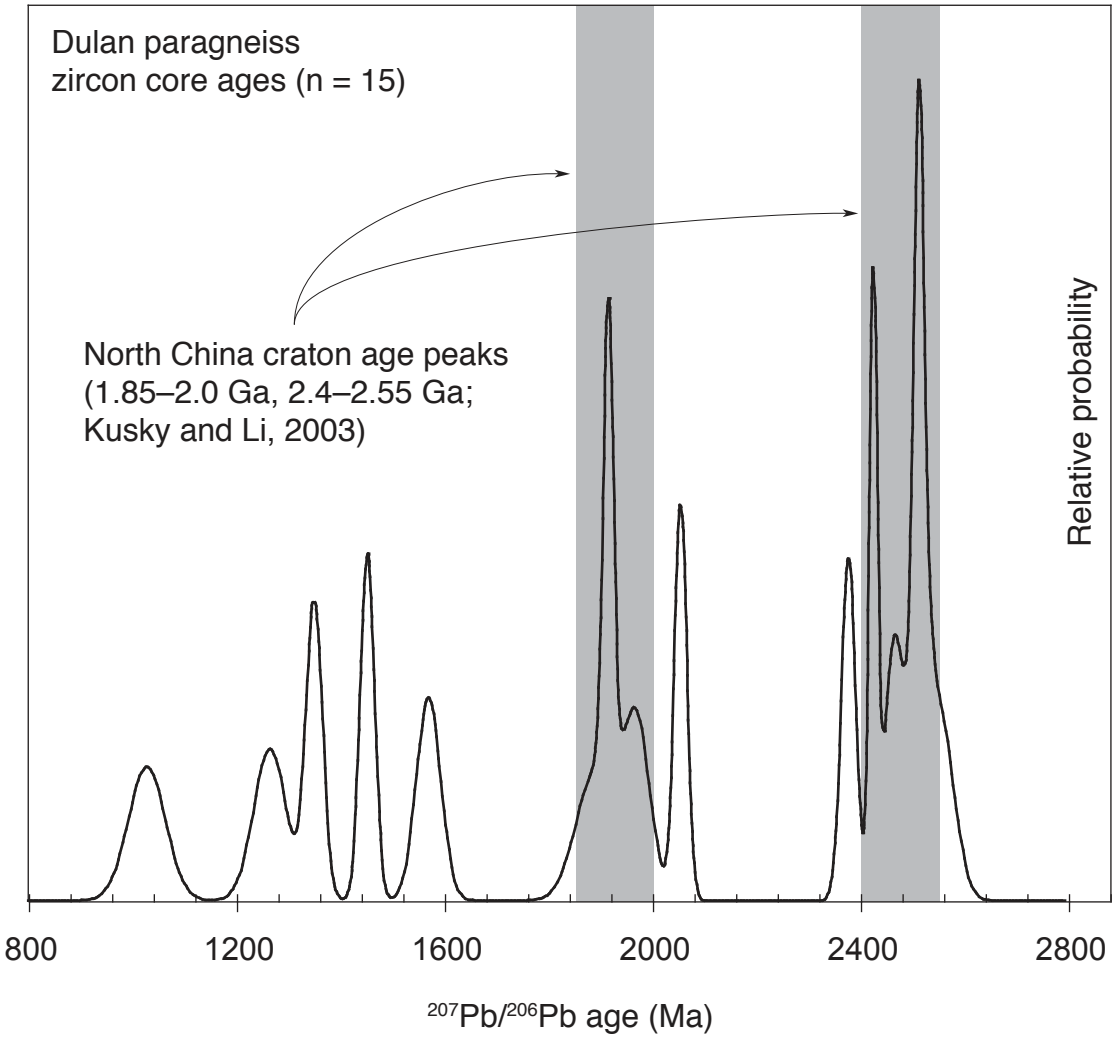
Dulan paragneiss
zircon core ages (n = 15)
North China craton age peaks
(1.85–2.0 Ga, 2.4–2.55 Ga;
Kusky and Li, 2003)
Relative probability
800
1200
1600
2000
2400
2800
207Pb/206Pb age (Ma)

Fig. 8

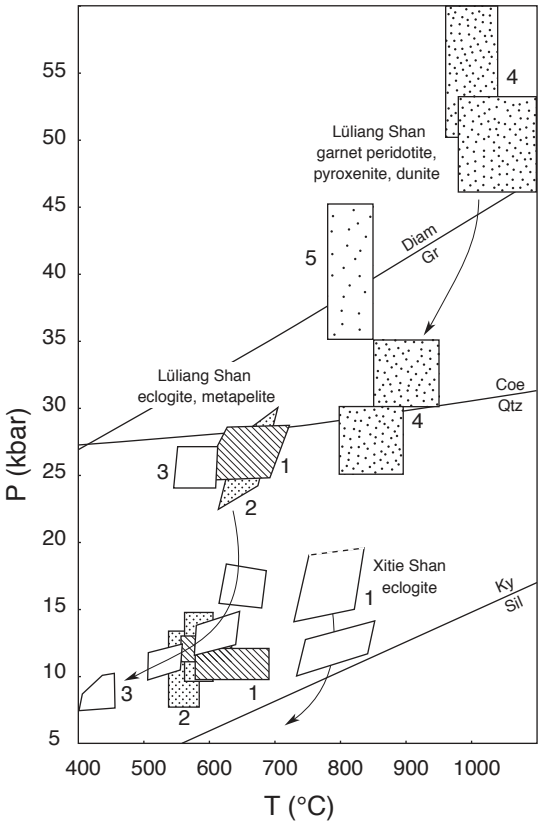
P (kbar)
T (°C)
55
50
45
40
35
30
25
20
15
10
5
400
500
600
700
800
900
1000
Lüliang Shan
garnet peridotite,
pyroxenite, dunite
Diam
Gr
Lüliang Shan
eclogite, metapelite
Coe
Qtz
Xitie Shan
eclogite
Ky
Sil
1
2
3
4
5

Fig. 9

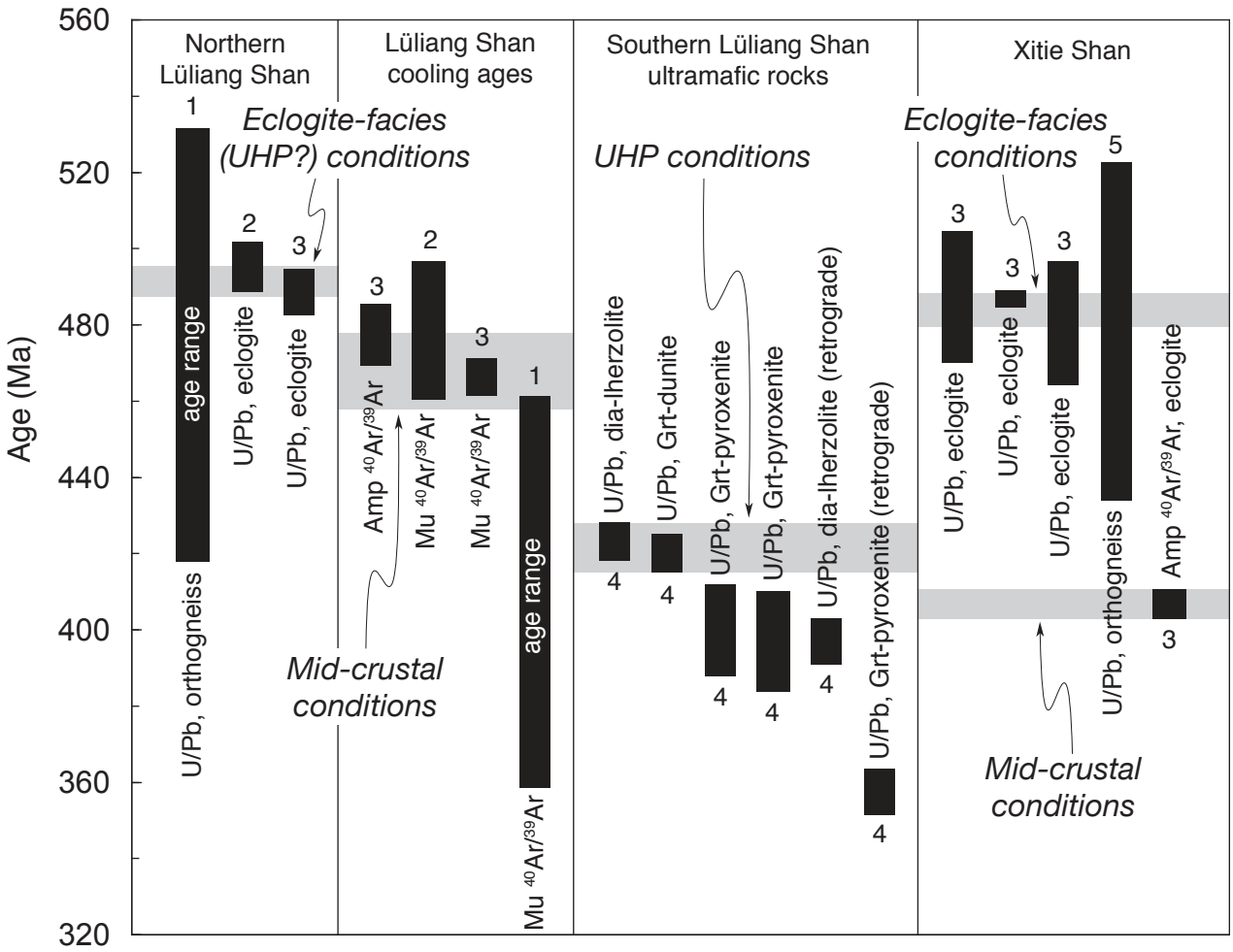
Age (Ma)
560
520
480
440
400
360
320
Northern Lüliang Shan
Lüliang Shan cooling ages
Southern Lüliang Shan ultramafic rocks
Xitie Shan
Eclogite-facies (UHP?) conditions
Mid-crustal conditions
UHP conditions
Eclogite-facies conditions
Mid-crustal conditions
age range
U/Pb, orthogneiss
U/Pb, eclogite
U/Pb, eclogite
Amp 40Ar/39Ar
Mu 40Ar/39Ar
Mu 40Ar/39Ar
age range
Mu 40Ar/39Ar
U/Pb, dia-lherzolite
U/Pb, Grt-dunite
U/Pb, Grt-pyroxenite
U/Pb, Grt-pyroxenite
U/Pb, dia-lherzolite (retrograde)
U/Pb, Grt-pyroxenite (retrograde)
U/Pb, eclogite
U/Pb, eclogite
U/Pb, eclogite
U/Pb, orthogneiss
Amp 40Ar/39Ar, eclogite

Fig. 10

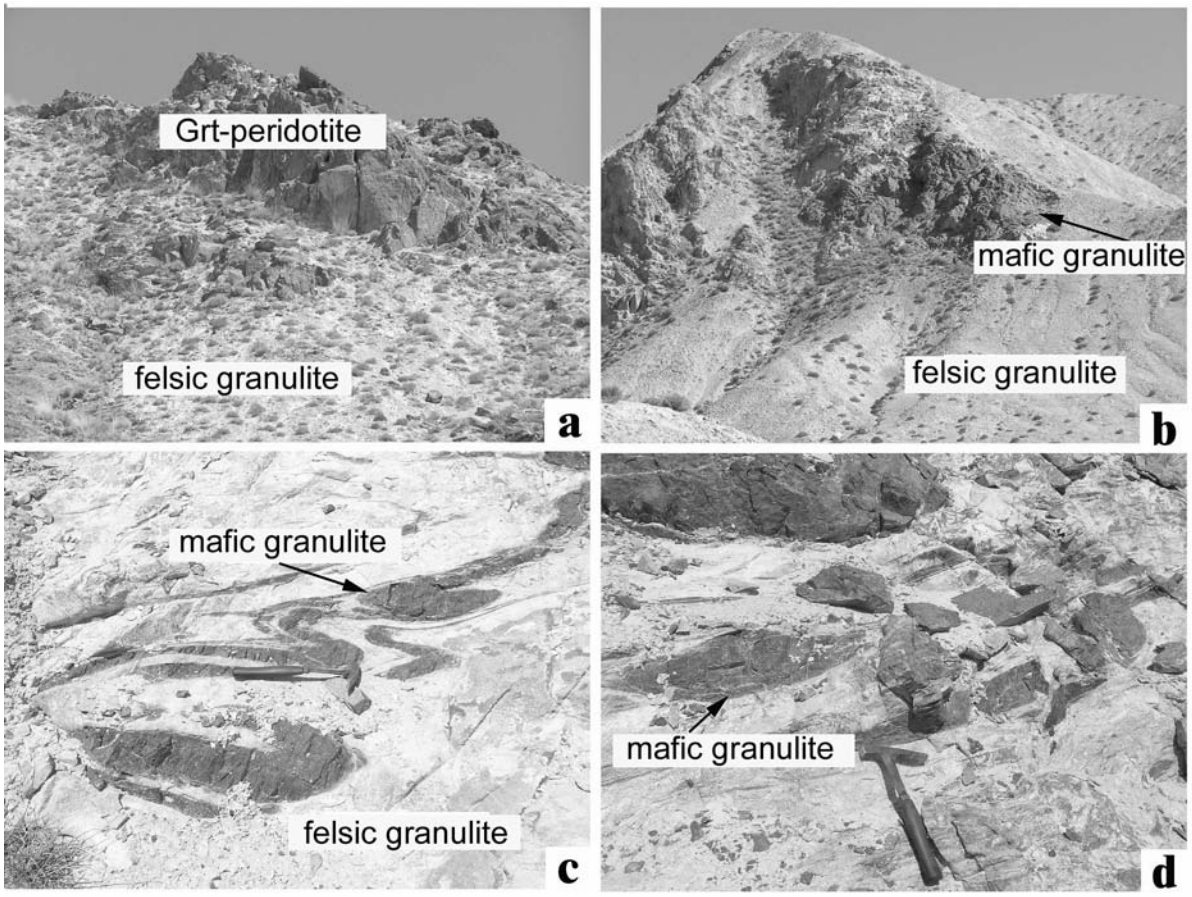
Grt-peridotite
felsic granulite
a
mafic granulite
felsic granulite
b
mafic granulite
felsic granulite
c
mafic granulite
d

Fig. 11

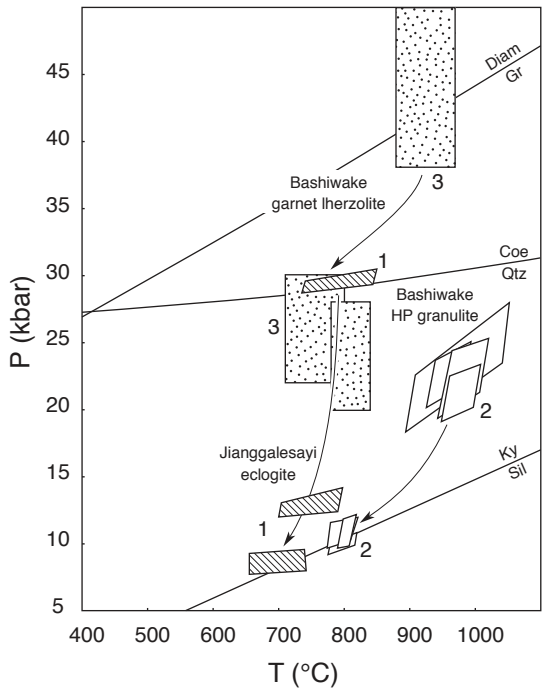
Diam
Gr
Bashiwake
garnet lherzolite
3
1
Coe
Qtz
Bashiwake
HP granulite
3
2
Jianggalesayi
eclogite
Ky
Sil
1
2
P (kbar)
T (°C)
45
40
35
30
25
20
15
10
5
400
500
600
700
800
900
1000

Fig. 12

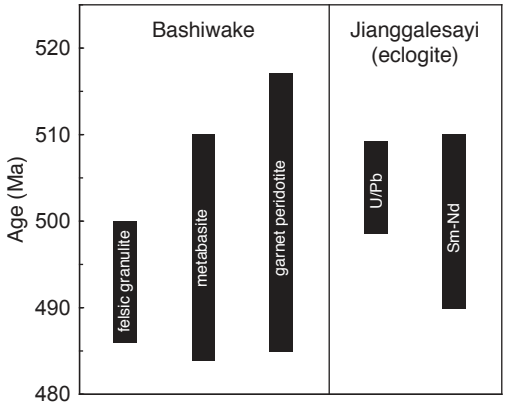
Bashiwake
Jianggalesayi
(eclogite)
520
510
500
490
480
Age (Ma)
felsic granulite
metabasite
garnet peridotite
U/Pb
Sm-Nd

Fig. 13

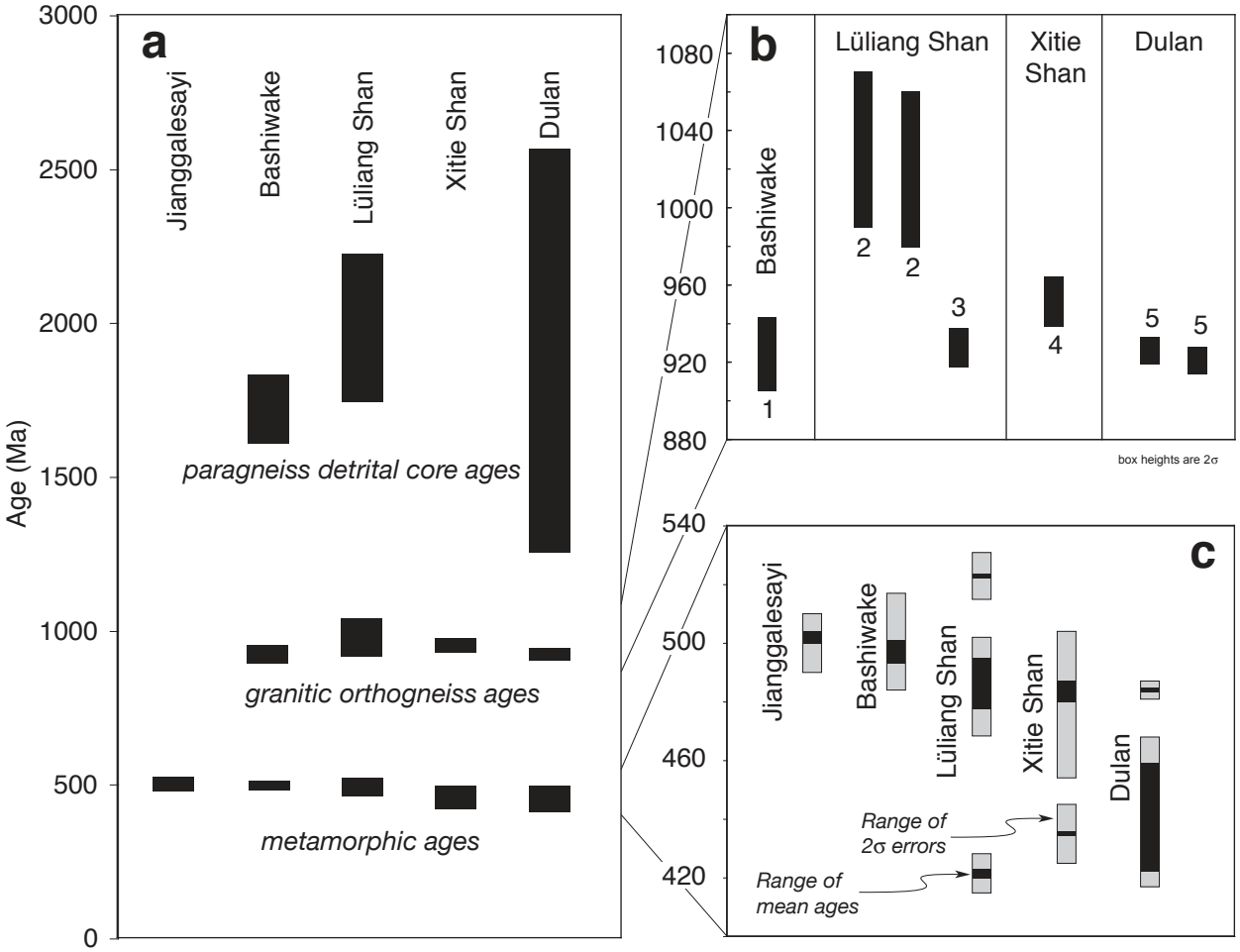
a
Jianggalesayi
Bashiwake
Lüliang Shan
Xitie Shan
Dulan
Age (Ma)
3000
2500
2000
1500
1000
500
0
paragneiss detrital core ages
granitic orthogneiss ages
metamorphic ages
b
Lüliang Shan
Xitie Shan
Dulan
Bashiwake
1080
1040
1000
960
920
880
540
500
460
420
1
2
2
3
4
5
5
box heights are 2σ
c
Jianggalesayi
Bashiwake
Lüliang Shan
Xitie Shan
Dulan
Range of 2σ errors
Range of mean ages

Figure 14

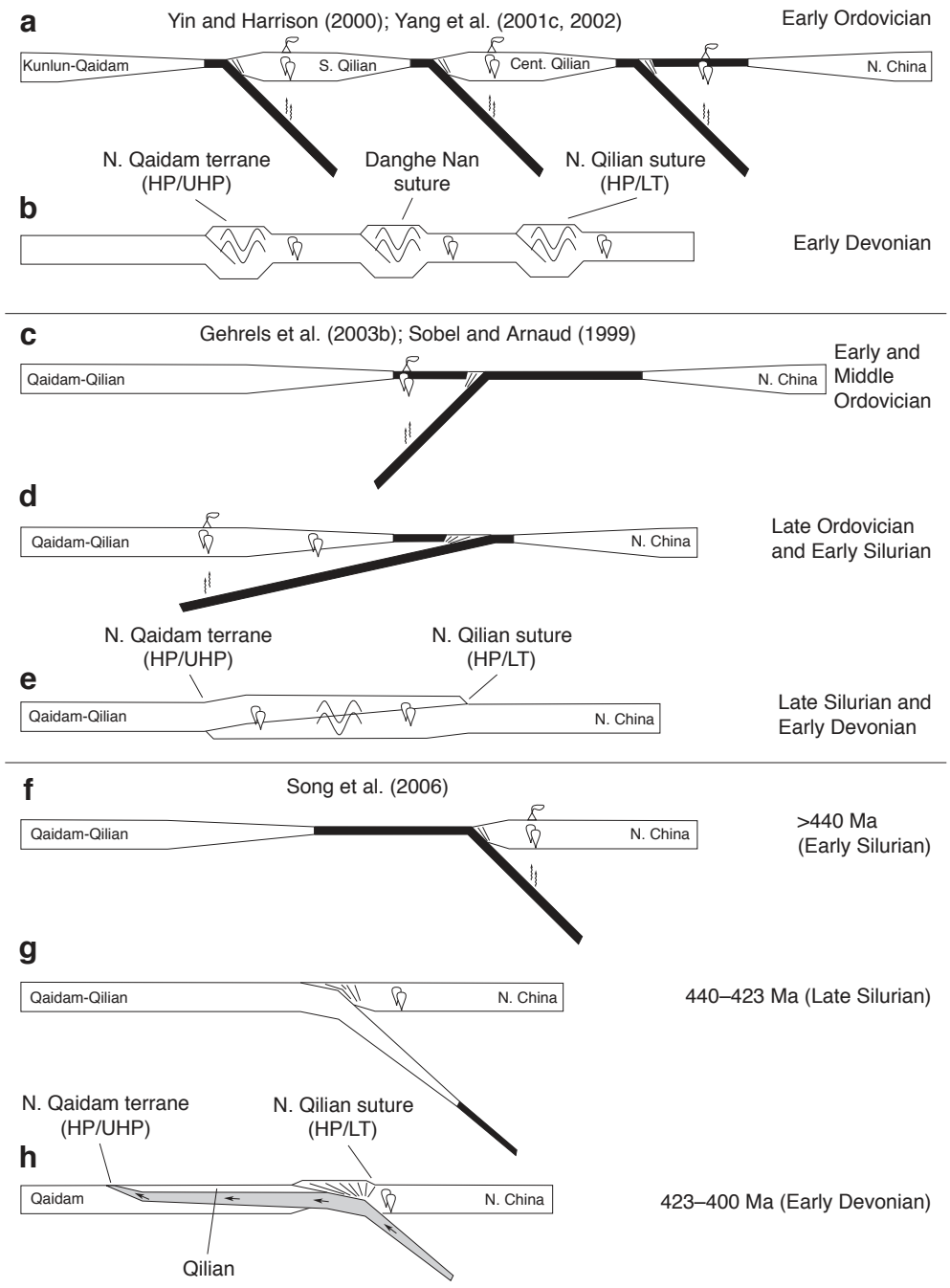
a
Yin and Harrison (2000); Yang et al. (2001c, 2002)
Early Ordovician
Kunlun-Qaidam
S. Qilian
Cent. Qilian
N. China
N. Qaidam terrane
(HP/UHP)
Danghe Nan
suture
N. Qilian suture
(HP/LT)
b
Early Devonian
c
Gehrels et al. (2003b); Sobel and Arnaud (1999)
Qaidam-Qilian
N. China
Early and
Middle
Ordovician
d
Qaidam-Qilian
N. China
Late Ordovician
and Early Silurian
N. Qaidam terrane
(HP/UHP)
N. Qilian suture
(HP/LT)
e
Qaidam-Qilian
N. China
Late Silurian and
Early Devonian
f
Song et al. (2006)
Qaidam-Qilian
N. China
>440 Ma
(Early Silurian)
g
Qaidam-Qilian
N. China
440–423 Ma (Late Silurian)
N. Qaidam terrane
(HP/UHP)
N. Qilian suture
(HP/LT)
h
Qaidam
N. China
423–400 Ma (Early Devonian)
Qilian

Fig. 15

Table 1: Thermobarometry from the North Qaidam and South Altyn HP/UHP terranes

sample#	location	rock type	reference	P (kbar)	T (°C)	assemblage	notes
Dulan (North Qaidam terrane)							
99Y308	none reported (north belt)	eclogite	Song et al., 2003b	31.7	687	Grt-Omp-Phe	peak stage
00Y104	none reported (north belt)	eclogite	Song et al., 2003b	28.7	631	Grt-Omp-Phe	peak stage
00Y108	none reported (north belt)	eclogite	Song et al., 2003b	29.6	665	Grt-Omp-Phe	peak stage
00Y219	map (approx; north belt)	paragneiss	Song et al., 2003a	>27		Coe inclusion in Zrn	
99Y80	none reported (south belt)	eclogite	Song et al., 2003b	28.6-32.6	729-768	Grt-Omp-Phe-Ky-Coe	peak stage
99Y81	none reported (south belt)	eclogite	Song et al., 2003a	>16	820-930	Grt-Cpx-Pl	granulite-facies retrograde stage
99Y201, 99Y213	none reported (south belt)	eclogite	Song et al., 2003b	18.6-19.8	874-948	Grt-Cpx-Pl-Qtz	granulite-facies retrograde stage
?	none reported (south belt)	eclogite	Song et al., 2003b	7-9	660-695	Grt-Amp-Ep-Bt-Pl-Qtz	amphibolite-facies retrograde stage
Xitieshan (North Qaidam terrane)							
QZ19-9	N37°22.90', E95°32.87'	eclogite	Zhang et al., 2005c	>14	730-830	Grt-Omp-Qtz	minimum P
QZ19-2	N37°24.51', E95°30.72'	eclogite	Zhang et al., 2005c	10-14	750-865	Grt-Cpx-Pl-Qtz	retrograde stage
Yuka/Lüliang Shan (North Qaidam terrane)							
97A25-1	N38°01.51', E94°52.71'	eclogite	Zhang et al., 2005c	10-14.6	567-644	Grt-Amp-Pl-Ep-Qtz	prograde stage
97A25-1	N38°01.51', E94°52.71'	eclogite	Zhang et al., 2005c	23-28	570-730	Grt-Omp-Phe	peak stage
97A26	N38°01.51', E94°52.71'	eclogite	Zhang et al., 2005c	9.7-12.8	586-674	Grt-Amp-Pl-Qtz	amphibolite-facies retrograde stage
QZ16-3-1	N37°53.08', E94°57.32'	eclogite	Zhang et al., 2005c	21.3-27.3	519-621	Grt-Omp-Phe-Qtz	peak stage
ZM-8	N37°58.54', E94°55.03'	metapelite	Zhang et al., 2004a	10.7±3.1	564±22	Grt-Chl-Cld-Phe-St-Qtz	prograde stage
ZM-8	N37°58.54', E94°55.03'	metapelite	Zhang et al., 2004a	23-31	615-700	Grt-Ky-Cld-Phe-Qtz	peak stage
ZM-8	N37°58.54', E94°55.03'	metapelite	Zhang et al., 2004a	12.2±2.6	581±20	Grt-Chl-Cld-Phe-St-Qtz	retrograde stage
LH101a	map (approx)	garnet peridotite	Yang et al., 1994	25±3	850±60	Grt-Cpx-Opx-Spl	
2C42	map (approx)	garnet lherzolite	Song et al., 2004	50-65	960-1040	Grt-Opx-Ol	
2C28	map (approx)	garnet dunite	Song et al., 2004	46-53	980-1130	Grt-Opx-Ol	
2C38 (?)	map (approx)	garnet pyroxenite	Song et al., 2004	30-35	850-950	Grt-Cpx-Opx	
2C42, 2C44, C305	map (approx)	garnet lherzolite	Song et al., 2005	50-65	960-1040	Grt-Opx-Ol	
?	map (approx)	garnet pyroxenite	Song et al., 2005	25-30	800-900	Grt-Cpx-Opx	
C305	map (approx)	garnet lherzolite	Song et al., 2005	>40		diamond inclusion in Zrn	
Y614	none reported	garnet peridotite	Zhang et al., 2004b	35-45	780-850	Grt-Cpx-Opx	
Bashiwake (South Altyn terrane)							
A761	N38°22.16', E88°37.31'	ky-felsic granulite	Zhang et al., 2005b	20-24.5	930-995	Grt-Ky-Fsp-Qtz	peak stage
A711	N38°22.16', E88°37.31'	mafic granulite	Zhang et al., 2005b	18.5-22.5	940-1005	Grt-Cpx-Fsp-Qtz	peak stage
A853	N38°21.75', E88°36.57'	mafic granulite	Zhang et al., 2005b	19.2-24	952-1012	Grt-Cpx-Pl-Qtz	peak stage
A851	N38°21.58', E88°37.06'	garnet peridotite	Zhang et al., 2005b	18.5-27.3	870-1050	Grt-Cpx-Opx-Ol	peak stage
	none reported	garnet lherzolite	Liu et al., 2002	38-51	880-970	Grt-Cpx-Opx	cores (peak)
	none reported	garnet lherzolite	Liu et al., 2002	22-30	710-800	Grt-Cpx-Opx	rims
	none reported	garnet lherzolite	Liu et al., 2002	20-28	780-840	Grt-Cpx-Opx	fine-grained matrix
A761	N38°22.16', E88°37.31'	ky-felsic granulite	Zhang et al., 2005b	9.3-10.6	802-830	Grt-Bt-Ky-Spl-Pl	retrograde stage
A711	N38°22.16', E88°37.31'	mafic granulite	Zhang et al., 2005b	9.6-12	782-819	Grt-Cpx-Pl-Qtz	retrograde stage
A853	N38°21.75', E88°36.57'	mafic granulite	Zhang et al., 2005b	9.4-12.2	802-822	Grt-Cpx-Opx-Pl-Qtz	retrograde stage
Jianggalesayi (South Altyn terrane)							
97A12-1	N38°00.23', E86°36.32'*	eclogite	Zhang et al., 2001	>15	731-811	Grt-Omp-Qtz	minimum P
97A12-1	N38°00.23', E86°36.32'*	eclogite	Zhang et al., 2001	28-30	820-850	Grt-Omp-Phe	peak stage
97A12-5	N38°00.45', E86°36.52'*	eclogite	Zhang et al., 2001	>15	665-880	Grt-Omp-Qtz	minimum P
97A12-5	N38°00.45', E86°36.52'*	eclogite	Zhang et al., 2002	28	730	Grt-Omp-Phe-Qtz	peak stage
97A12-1	N38°01.05', E86°36.25'*	eclogite	Zhang et al., 2001	11-14	670-800	Grt-Cpx-Pl-Qtz	granulite-facies retrograde stage
97A21a	N38°01.35', E86°36.18'*	eclogite	Zhang et al., 2001	6.3-7.6	730	Grt-Amp-Pl-Qtz	amphibolite-facies retrograde stage
97A14c	N38°00.55', E86°36.46'*	eclogite	Zhang et al., 2001	7.8-9.5	638-738	Grt-Amp-Pl-Qtz	amphibolite-facies retrograde stage

*approximate

Table 2: Geochronology from the North Qaidam and South Altyn HP/UHP terranes

sample#	location	rock type	age type	reference	age (Ma, ±2σ)	notes
Dulan (North Qaidam terrane)						
ZD21G	N36°36.25', E98°28.44'	paragneiss	zrc U/Pb	Mattinson et al., 2005	426.1 ± 3.9	SHRIMP, n=11, MSWD=1.2
ZD21G	N36°36.25', E98°28.44'	paragneiss	zrc U/Pb	C.G. Mattinson, unpbl.	1265 - 2465	SHRIMP Pb/Pb; cores, <35% discordant, n=2
D12H	N36°36.56', E98°27.36'	paragneiss	zrc U/Pb	C.G. Mattinson, unpbl.	1916 - 2425	SHRIMP Pb/Pb; cores, <35% discordant, n=3
ZD22A	N36°36.06', E98°28.76'	paragneiss	zrc U/Pb	C.G. Mattinson, unpbl.	1452 - 2554	SHRIMP Pb/Pb; cores, <35% discordant, n=6
2D132	N36°36.75', E98°26.33'	coe-paragneiss	zrc U/Pb	Song et al., 2006	423 ± 6	SHRIMP, n=18, MSWD=0.4; coe-bearing grains are 423±17, 431±11, 426±12, 429±12
2D132	N36°36.75', E98°26.33'	coe-paragneiss	zrc U/Pb	Song et al., 2006	403 ± 9	SHRIMP, n=6, MSWD=0.19; rims
01Y132	none reported	coe-paragneiss	zrc U/Pb	Yang et al., 2005	452 ± 13.8	SHRIMP, average includes coe-bearing grain (440±17) and 2 cores (467 ± 8.9, 448 ± 8.7); no data, location
01Y132	none reported	coe-paragneiss	zrc U/Pb	Yang et al., 2005	419 ± 13.4	SHRIMP, single rim spot, no data, location
01Y469	none reported	coe-paragneiss	zrc U/Pb	Yang et al., 2005	433.5 ± 6.6	SHRIMP, n=11, MSWD=4.8; two spots on coe-bearing grains are 438.8 ± 2.6, 426.8 ± 3.7, no data, location
01Y469	none reported	coe-paragneiss	zrc U/Pb	Yang et al., 2005	919 - 2423	SHRIMP, 9 cores; excluded 2 younger, discordant analyses; no data, location
D7B	N36°31.07', E98°36.75'	orthogneiss	zrc U/Pb	Mattinson et al., 2006	926.6 ± 6.9	SHRIMP, n=9, MSWD=0.52
D15D	N36°35.94', E98°28.45'	orthogneiss	zrc U/Pb	Mattinson et al., 2006	921.4 ± 7	SHRIMP, n=11, MSWD=1.1
	none reported	orthogneiss	zrc U/Pb	Yang et al., 2001b	932 - 1011	no errors, data, location
D12L	N36°36.67', E98°27.49'	g-amphibolite	zrc U/Pb	Mattinson et al., 2005	1880 ± 79	SHRIMP upper intercept, MSWD=5.5
D12L	N36°36.67', E98°27.49'	g-amphibolite	zrc U/Pb	Mattinson et al., 2005	443.5 ± 6.8	SHRIMP, n=10, MSWD=1.1
D12N	N36°36.67', E98°27.49'	g-bi-amph gneiss	zrc U/Pb	Mattinson et al., 2005	2438 ± 29	SHRIMP upper intercept, MSWD=5.7
D12N	N36°36.67', E98°27.49'	g-bi-amph gneiss	zrc U/Pb	Mattinson et al., 2005	452 ± 30	SHRIMP lower intercept, MSWD=5.7
D3F	N36°36.35', E98°26.24'	eclogite	zrc U/Pb	Mattinson et al., in press	422 ± 4.3	SHRIMP, n=10, MSWD=0.83; eclogite-facies (inclusions, REE)
D5A	N36°36.39', E98°26.33'	eclogite	zrc U/Pb	Mattinson et al., in press	433 - 474	SHRIMP; cores, prograde metamorphic, pre-eclogite (inclusions, REE)
D5A	N36°36.39', E98°26.33'	eclogite	zrc U/Pb	Mattinson et al., in press	448.9 ± 2.2	SHRIMP, n=19, MSWD=2.0; eclogite-facies (inclusions, REE)
D5B	N36°36.39', E98°26.33'	eclogite	zrc U/Pb	Mattinson et al., in press	441.7 ± 4.1	SHRIMP, early eclogite facies (steep HREE, inclusions); n=5, MSWD=2.2
D5B	N36°36.39', E98°26.33'	eclogite	zrc U/Pb	Mattinson et al., in press	432.5 ± 4.7	SHRIMP, later eclogite facies (flat HREE, inclusions); n=7, MSWD=2.8
2D155	N36°35.40', E98°25.03'	eclogite	zrc U/Pb	Song et al., 2006	457 ± 7	SHRIMP, n=15, MSWD=0.91; Grt, Omp, Rt inclusions

Table 2: (continued)

sample#	location	rock type	age type	reference	age (Ma, ±2σ)	notes
2D155	N36°35.40', E98°25.03'	eclogite	zrc U/Pb	Song et al., 2006	426 ± 24	SHRIMP, single rim spot
99Y115	same as 2D155?	eclogite	zrc U/Pb	Yang et al., 2002	443 - 495	no errors, data, or location
	none reported; south belt	eclogite	zrc U/Pb	Yang et al., 2001b	462 - 487	no errors, data, or location
	none reported; south belt	eclogite	zrc U/Pb	Yang et al., 2001b	968 - 1097	protolith; no errors, data, location
QD03	on map; south belt	eclogite	zrc U/Pb	Lu, 2003	484 ± 3	TIMS, n=6; lower intercept 497±10, upper inercept 2055±85, n=9
QD03	on map; south belt	eclogite	zrc U/Pb	Lu, 2003	1482	TIMS Pb/Pb age of oldest, discordant analysis
99Y115	same as 2D155?	eclogite	Sm/Nd	Yang et al., 2002	457.7 ± 3.3	Grt-Omp-WR, effectively 2-point isochron; no data or location
99Y115	same as 2D155?	eclogite	Sm/Nd	Song et al., 2003a	458 ± 10	Grt-Omp-WR, effectively 2-point isochron, exact same data as Yang et al., 2002?
99Y313	same as 2D155?	eclogite	Sm/Nd	Song et al., 2003a	459 ± 2.6	Grt-Omp-WR, no location
99Y205	none reported; south belt	eclogite	Sm/Nd	Song et al., 2003a	497 ± 87	Grt-Omp-WR, no location
	none reported; north belt	eclogite	Sm/Nd	Yang et al., 2001b	442	no errors, data, location
	none reported; south belt	eclogite	Sm/Nd	Yang et al., 2001b	496	no errors, data, location
9Y117	N36°35.40', E98°25.05'	orthogneiss	mu Ar/Ar	Song et al., 2006	401.5 ± 1.6	plateau, 7 of 11 steps
CL9940	on map	granite	zrc U/Pb	Wu et al., 2004	397 ± 3	SHRIMP, n=14, MSWD=0.42; I/S-type, syn-collisional
Xitie Shan (North Qaidam terrane)						
XTS-1	N37°24.10', E95°30.95'	paragneiss	zrc U/Pb	J.X. Zhang unpbl.	>1100	SHRIMP, core
XTS-1	N37°24.10', E95°30.95'	paragneiss	zrc U/Pb	J.X. Zhang unpbl.	~900	SHRIMP; mantles; metamorphic (Th/U<0.1, CL cloudy pattern)
XTS-1	N37°24.10', E95°30.95'	paragneiss	zrc U/Pb	J.X. Zhang unpbl.	435 - 437	SHRIMP; rims
QZ19-3-1	N37°24.51', E95°30.72'	orthogneiss	zrc U/Pb	Zhang et al., in press	952 ± 13	TIMS upper intercept, n=4; magmatic
QZ19-3-2	N37°24.51', E95°30.72'	orthogneiss	zrc U/Pb	Zhang et al., in press	478 ± 44	TIMS lower intercept, n=4; metamorphic
QZ19-2	N37°24.51', E95°30.72'	eclogite	zrc U/Pb	Zhang et al., 2005c	486.4 ± 2.3	TIMS, n=3, MSWD=0.04
QZ19-9	N37°22.90', E95°32.87'	eclogite	zrc U/Pb	Zhang et al., 2005c	487 ± 17	TIMS, n=1
QZ19-9	N37°22.90', E95°32.87'	eclogite	zrc U/Pb	Zhang et al., 2005c	807 ± 48	TIMS upper intercept, MSWD=0.86
QZ19-9	N37°22.90', E95°32.87'	eclogite	zrc U/Pb	Zhang et al., 2005c	480 ± 16	SHRIMP, n=7, MSWD=1.3
QZ19-9	N37°22.90', E95°32.87'	eclogite	zrc U/Pb	Zhang et al., 2005c	1098 ± 84	SHRIMP Pb/Pb; cores, discordant
QZ19-9	N37°22.90', E95°32.87'	eclogite	zrc U/Pb	Zhang et al., 2005c	875 ± 39	SHRIMP Pb/Pb; cores, discordant
QZ19-9	N37°22.90', E95°32.87'	eclogite	Sm/Nd	Zhang et al., 2005c	436 ± 49	Grt-Omp-WR, cooling age

Table 2: (continued)

sample#	location	rock type	age type	reference	age (Ma, ±2σ)	notes
QZ19-2	N37°24.51', E95°30.72'	eclogite	amp Ar/Ar	Zhang et al., 2005c	407 ± 4	isochron
Yuka/Lüliang Shan (North Qaidam terrane)						
2C126	N37°59.22', E94°53.40'	paragneiss	zrc U/Pb	Song et al., 2006	2216 ± 18	SHRIMP Pb/Pb; cores, oldest spot
2C126	N37°59.22', E94°53.40'	paragneiss	zrc U/Pb	Song et al., 2006	1756 ± 8	SHRIMP; cores, ~upper intercept
2C126	N37°59.22', E94°53.40'	paragneiss	zrc U/Pb	Song et al., 2006	918 ± 25	SHRIMP; cores, ~lower intercept
ZM5-5.4	N37°39.40', E95°21.07'	orthogneiss	zrc U/Pb	J.X. Zhang unpbl.	1300 - 2500	SHRIMP; cores
ZM5-5.4	N37°39.40', E95°21.07'	orthogneiss	zrc U/Pb	J.X. Zhang unpbl.	~900	SHRIMP; mantles; magmatic (Th/U>0.1,oscillatory-zoned CL)
ZM5-5.4	N37°39.40', E95°21.07'	orthogneiss	zrc U/Pb	J.X. Zhang unpbl.	448	SHRIMP; rims
GA211	N37°56.15', E94°58.75'	orthogneiss	zrc U/Pb	Gehrels et al., 2003b	928 ± 10	magmatic; TIMS upper intercept, n=10, MSWD=1.1
		(ortho?)gneiss	zrc U/Pb	Yang et al., 2001b	1022	no errors, data, location
		orthogneiss	zrc U/Pb	J.X. Zhang unpbl.	900 - 1000	magmatic
N32-2	N37°59.61', E94°54.20'*	orthogneiss	zrc U/Pb	Wan et al., 2001	1030 ± 40	mu granite, no data
97A6-7	N38°00.05', E94°54.85'*	orthogneiss	zrc U/Pb	Wan et al., 2001	1020 ± 40	mu granite, no data
various		orthogneiss	zrc U/Pb	Menold et al. 2004	425±7 - 523±8	SIMS, ages differ among blocks
		ophiolite gabbro	zrc U/Pb	Menold et al. 2004	545.5 ± 6	
		g-amphibolite	zrc U/Pb	Yang et al., 2001b	440	
QZ16-3-1	N37°53.08', E94°57.32'	eclogite	zrc U/Pb	Zhang et al., 2005c	488 ± 6	TIMS, n=3, MSWD=0.33
QZ16-3-1	N37°53.08', E94°57.32'	eclogite	zrc U/Pb	Zhang et al., 2005c	844 ± 9	TIMS Pb/Pb, discordant
QZ16-3-1	N37°53.08', E94°57.32'	eclogite	zrc U/Pb	Zhang et al., 2005c	923 ± 5	TIMS Pb/Pb, discordant
97A25-1	N38°01.51', E94°52.71'	eclogite	zrc U/Pb	Zhang et al., 2000	494.6 ± 6.5	TIMS, n=3, MSWD=0.71
C305	map (approx)	garnet lherzolite	zrc U/Pb	Song et al., 2005	731 - 1093	SHRIMP Pb/Pb, n=2, inherited cores
C305	map (approx)	garnet lherzolite	zrc U/Pb	Song et al., 2005	457 ± 22	SHRIMP, n=5, MSWD=3.4; cores, magmatic (?, but could be prograde metamorphic; REE)
C305	map (approx)	garnet lherzolite	zrc U/Pb	Song et al., 2005	423 ± 5	SHRIMP, n=13, MSWD=0.56; UHP, one zrc contains diamond inclusion
C305	map (approx)	garnet lherzolite	zrc U/Pb	Song et al., 2005	397 ± 6	SHRIMP, n=10, MSWD=0.31; rims, exhumation-related?
C305	map (approx)	garnet lherzolite	zrc U/Pb	Song et al., 2005	349 - 367	SHRIMP, n=4; outer rims, reflects post-orogenic thermal events?
2C39	map (approx)	garnet dunite	zrc U/Pb	Song et al., 2005	446 ± 13	SHRIMP, n=4, MSWD=0.67; cores, magmatic or prograde metamorphic

Table 2: (continued)

sample#	location	rock type	age type	reference	age (Ma, ±2σ)	notes
2C39	map (approx)	garnet dunite	zrc U/Pb	Song et al., 2005	420 ± 5	SHRIMP, n=15, MSWD=0.39; metamorphic, Grt + Ol inclusions, REE
2C39	map (approx)	garnet dunite	zrc U/Pb	Song et al., 2005	391 - 405	SHRIMP, n=3; rims
2C12	map (approx)	garnet pyroxenite	zrc U/Pb	Song et al., 2005	443 ± 17	SHRIMP, core, single spot
2C12	map (approx)	garnet pyroxenite	zrc U/Pb	Song et al., 2005	397 ± 13	SHRIMP, n=9, MSWD=1.5, metamorphic, post-UHP?
2C78	map (approx)	garnet pyroxenite	zrc U/Pb	Song et al., 2005	400 ± 12	SHRIMP, n=10, MSWD=3.7, metamorphic (REE), post-UHP?
2C78	map (approx)	garnet pyroxenite	zrc U/Pb	Song et al., 2005	358 ± 6	SHRIMP, n=5, MSWD=0.67; rims, retrograde event
	none reported	garnet peridotite	zrc U/Pb	Yang et al., 2002	436 - 487	no uncertanties, data, or location
	N38°01.42', E94°55.69'*	orthogneiss	mu Ar/Ar	Zhang et al., 2000	478 ± 18	isochron, MSWD=23, excess Ar
various		orthogneiss	mu Ar/Ar	Menold et al. 2004	460 - 360	
	none reported	(ortho?)gneiss	mu Ar/Ar	Yang et al., 2001b	477	no errors, data, location
97A25-1	N38°01.51', E94°52.71'	eclogite	amp Ar/Ar	Zhang et al., 2005c	477 ± 8	isochron
97A25-1	N38°01.51', E94°52.71'	eclogite	mu Ar/Ar	Zhang et al., 2005c	466 ± 5	isochron
K554	map (approx)	granite	zrc U/Pb	Wu et al., 2002	446 ± 7.7	SHRIMP, n=7; S-type syn-collisional
GA213	N37°57.27', E95°21.23'	granite	zrc U/Pb	Gehrels et al., 2003b	442 ± 4	TIMS, n=4
Bashiwake (South Altyn terrane)						
A761	N38°22.16', E88°37.31'	Ky- felsic granulite	zrc U/Pb	Zhang et al., 2005b	493 ± 7	SHRIMP, n=11, MSWD=3.0; metamorphic
A761	N38°22.16', E88°37.31'	Ky- felsic granulite	zrc U/Pb	Zhang et al., 2005b	1722 ± 99	SHRIMP Pb/Pb, n=1; inherited detrital grain
A712	N38°22.12', E88°37.81'*	orthogneiss	zrc U/Pb	C.G. Mattinson, unpbl.	925 ± 19	SHRIMP, n=14, MSWD=0.77; magmatic (REE)
A841	N38°21.58', E88°37.06'	Spr-metabasite	zrc U/Pb	Zhang et al., 2005b	497 ± 13	SHRIMP, n=12, MSWD=0.96; metamorphic Th/U, Grt, Cpx, Rt inclusions
A851	N38°21.58', E88°37.06'	garnet peridotite	zrc U/Pb	Zhang et al., 2005b	501 ± 16	SHRIMP, n=10, MSWD=3; metamorphic, Opx inclusions
Jianggelesayi (South Altyn terrane)						
97A12-1	N38°00.23', E86°36.32'*	eclogite	zrc U/Pb	Zhang et al., 2001	503.9 ± 5.3	TIMS, n=4, MSWD=0.204
97A12-1	N38°00.23', E86°36.32'*	eclogite	Sm/Nd	Zhang et al., 2001	500 ± 10	Grt-Omp-WR, MSWD=1.41

*approximate